CXCR5+ follicular cytotoxic T cells control viral infection in B cell follicles

Leong, Yew Ann; Chen, Yaping; Ong, Hong Sheng; Wu, Di; Man, Kevin; Deleage, Claire; Minnich, Martina; Meckiff, Benjamin; Wei, Yunbo; Hou, Zhaohua; Zotos, Dimitra; Fenix, Kevin A; Atnerkar, Anurag; Preston, Simon; Chipman, Jeffrey G; Beilman, Greg J; Allison, Cody C; Sun, Lei; Wang, Peng; Xu, Jiawei

Document Version
Peer reviewed version

[Link to publication on Research at Birmingham portal](#)

CXCR5[+] follicular cytotoxic T cells control viral infection in B cell follicles

Yew Ann Leong[1], Yaping Chen[1], Hong Sheng Ong[1], Di Wu[2], Kevin Man[3,4], Claire Deleage[5], Martina Minnich[6], Benjamin J Meckiff[7], Yunbo Wei[8], Zhaohua Hou[8], Dimitra Zotos[3,4], Kevin A Fenix[9], Anurag Atnerkar[1], Simon Preston[3,4], Jeffrey G Chipman[10], Greg J Beilman[10], Cody C Allison[3,4], Lei Sun[11], Peng Wang[11], Jiawei Xu[12], Jesse G Toe[3,4], Hao K Lu[13], Yong Tao[14], Umaimainthan Palendira[15], Alexander L Dent[16], Alan L Landay[17], Marc Pellegrini[3,4], Iain Comerford[9], Shaun R McColl[9], Timothy W Schacker[18], Heather M. Long[7], Jacob D Estes[5], Meinrad Busslinger[6], Gabrielle T Belz[3,4], Sharon R Lewin[13,19], Axel Kallies[3,4]*, Di Yu[1,20]*

[1]Infection and Immunity Program, Monash Biomedicine Discovery Institute and Department of Biochemistry and Molecular Biology, Monash University, Victoria, Australia.

[2]School of Dentistry, The University of North Carolina at Chapel Hill, NC, United States of America.

[3]The Walter and Eliza Hall Institute of Medical Research, Parkville, Victoria, Australia.

[4]The Department of Medical Biology, University of Melbourne, Parkville, Victoria, Australia

[5]AIDS and Cancer Virus Program, Leidos Biomedical Research, Inc., Frederick National Laboratory for Cancer Research, Frederick, MD, United States of America.

[6]Research Institute of Molecular Pathology, Vienna Biocenter, Vienna, Austria.

[7]Institute of Immunology and Immunotherapy, Centre for Human Virology and Cancer Immunology and Immunotherapy Centre, University of Birmingham, United Kingdom

[8]Shandong Analysis and Test Center, Shandong Academy of Sciences, Jinan, Shandong, China.

[9]Department of Molecular and Cellular Biology, School of Biological Sciences, University of Adelaide, Adelaide, South Australia, Australia.

[10]Department of Surgery, University of Minnesota, Minneapolis, MN, United States of America

[11]Department of Pathology, Beijing Ditan Hospital, Capital Medical University, Beijing, China

[12]Department of Biostatistics, Gillings School of Global Public Health, University of North Carolina, Chapel Hill, NC, United States of America

[13]The Peter Doherty Institute for Infection and Immunity, University of Melbourne and Royal Melbourne Hospital, Melbourne, Australia.

[14]Department of Ophthalmology, Beijing Chaoyang Hospital, Capital Medical University, Beijing, China

[15]Centenary Institute, Newtown, New South Wales, Australia

[16]Department of Microbiology and Immunology, Indiana University School of Medicine, Indianapolis, Indiana, United States of America

[17]Department of Immunology/Microbiology, Rush University Medical Center, Chicago, Illinois, United States.

[18]Department of Medicine, University of Minnesota, Minneapolis, MN, United States of America

[19]Department of Infectious Diseases, The Alfred and Monash University, Melbourne, Australia

[20]Centre for Inflammatory Diseases, School of Clinical Sciences, Monash University, Victoria 3800, Australia.

*Correspondence to: di.yu@moansh.edu and kallies@wehi.edu.au.

In response to infection, antigen-specific CD8^{+} T cells are primed in the T cell zone of secondary lymphoid organs and differentiate into cytotoxic effector T (T_C) cells[1]. Concurrently, CD4^{+} T cells differentiate into follicular helper T (T_{FH}) cells that localize to B cell follicles and promote protective antibody responses[2]. During unresolved infections, however, some viruses including human immunodeficiency virus (HIV) or Epstein–Barr virus (EBV) escape immune control and persist in T_{FH} cells and B cells, respectively[3-8]. Exclusion of Tc cells from B cell follicles is thought to be a major mechanism of immune evasion[9-11]. New strategies are therefore needed to eradicate infected cells in follicles for a permanent cure. Using mouse infection models and human samples, we here identify a specialized group of T_C cells expressing the chemokine receptor CXCR5 that can selectively enter B cell follicles and eradicate infected T_{FH} and B cells. We demonstrate that differentiation of these cells, which we term follicular cytotoxic T (T_{FC}) cells, requires the transcription factors Bcl6, E2A and Tcf1, whereas the transcriptional regulators Blimp1, Id3 and Id2 inhibit their development. We demonstrate that Blimp1 and E2A directly regulate *Cxcr5* expression, and together with Bcl6 and Tcf1 form a transcriptional circuit that guides T_{FC} differentiation. The identification of a follicular subset of T_C cells has far-reaching implications for developing better strategies for the control of infections that target B cells and T_{FH} cells and for the eradication of B cell-derived malignancies.

Coordinate differentiation of distinct effector populations of T_C cells is required for efficient elimination of infected or cancerous cells. Differentiation of T_C is driven by a network of transcription factors, most prominently by T-bet, Blimp1 and Id2, which regulate differentiation of effector Tc cells[12,13]. In addition to the acquisition of cytotoxic effector function, migration to the site of infection or tumour growth is a prerequisite for efficient function of Tc cells. The entry of Tc cells in lymphoid and non-lymphoid tissues is well studied[1]; however, surprisingly, little is known about the ability of Tc cells to enter B cell follicles and control infection at this site. Although some studies suggest that Tc cells are excluded from entry into B cell follicles[9,11], CXCR5$^+$ CCR7$^-$ T_C cells were reported to position in tonsil B cell follicles[14]. In line with this finding, we found significant numbers of T_C cells in B cell follicles of lymph nodes from HIV-infected individuals naïve to treatment (**Fig. 1A**). Importantly, some follicular T_C cells localized in close proximity to HIV-infected cells (**Fig. 1B**), suggesting they may play a role in controlling the infection in B cell follicles. Localization of T cells is regulated by the expression of multiple chemotactic receptors. Naïve T cells express C-C chemokine receptor type 7 (CCR7) and localize to the T cell zone. However, upon antigen-stimulation CCR7 is down-regulated, and CD4$^+$ T cells migrate to the T-B border where they can upregule CXCR5 and differentiate into T_{FH} cells that enter the B cell follicles[15]. We hypothesized that a similar mechanism might also govern the follicular positioning of T_C cells in infection. Indeed, we identified CXCR5 expression in a substantial percentage of CD45RA$^-$CCR7$^-$ effector T_C cells in lymph nodes from HIV-infected individuals (**Fig. 1C**).

To examine how Tc cells gain access to B cell follicles during viral infection and contribute to virus control, we made use of the DOCILE strain of the lymphocytic

choriomeningitis virus (LCMV), which causes a chronic infection in mice that shares characteristics with HIV infection[16]. We also utilized T-cell receptor (TCR) transgenic CD8$^+$ T cells (P14) specific for the LCMV epitope gp$_{33\text{-}41}$ (ref. 17), which we transferred into recipient mice before LCMV infection. On day 8 post-infection, P14 cells were observed not only in the T cell zone but also in B cell follicles where they persisted beyond day 21 post-infection (**Fig. 1D**). We also observed endogenous CD8$^+$ T cells in B cell follicles in LCMV-infected mice that did not receive P14 cells (**Fig. S1**). Both transferred P14 cells and endogenous activated T$_C$ cells showed minimal expression of CCR7 (**Fig. S2A**). CXCR5 expression was detected on approximately 20% of P14 cells and 10% of endogenous LCMV-specific CD8$^+$ T cells (**Fig. 1E** and **S2B**). The percentage of the CXCR5$^+$ subset amongst the transferred P14 cells increased from day 8 to day 15 and remained high at least until day 35 post-infection (**Fig. 1F**). Upregulation of CXCR5 was also detected on OT-I CD8$^+$ T cells that expressed a transgenic TCR specific for the ovalbumin (OVA) epitope 257-264 (ref. 18) in mice that were infected with OVA-expressing influenza virus or immunized with OVA in complete freund's adjuvant (**Fig. S3**). Importantly, *Cxcr5$^{-/-}$* P14 cells were severely impaired in their ability to enter B cell follicles in comparison to their wildtype counterparts (**Fig. 1G**). Similar to LCMV and influenza virus, infection of mice with B cell-tropic Murid Herpesvirus-4 (MuHV-4) resulted in the generation of CXCR5$^+$ T$_{FC}$ cells (**Fig. 1H**). Finally, CXCR5 expression was also confirmed on human T$_C$ cells specific for EBV (also known as human herpesvirus 4, HHV-4) in tonsils from individuals previously infected with EBV (**Fig. 1I**). These data demonstrate that CXCR5 is expressed on mouse and human T$_{FC}$ cells localized in B cell follicles.

LCMV preferentially replicates in myeloid cells, but also infects CD4^{+} T cells[19]. Intracellular staining with an antibody (VL4) specific to the LCMV nucleoprotein (NP) can be used to quantify the amount of viral particles in cells[19,20]. LCMV-infected mice harboured significant numbers of virus-infected CD4^{+} T cells (**Fig. S4**). In addition, we observed the presence of LCMV in T_{FH} cells in B cell follicles and non-T_{FH} cells in T cell zones (**Fig. 2A**). At day 15 post-infection, T_{FH} cells showed higher infection rates than non-T_{FH} cells (**Fig. 2B** and **C**), which was confirmed by quantification of LCMV RNA (**Fig. S5**). To test whether T_{FC} cells are essential to specifically control infection of T_{FH} cells, we adoptively transferred SMARTA CD4^{+} T cells expressing a transgenic TCR specific for the LCMV epitope gp_{66-77} (ref. 21), together with either $Cxcr5^{+/+}$ or $Cxcr5^{-/-}$ P14 cells into mice and infected them with LCMV (**Fig. S6A**). In order to avoid competition with endogenous T cells, we used mice carrying an irrelevant TCR-transgene (OT-I) as recipients. As expected, upon LCMV infection, SMARTA cells differentiated into both T_{FH} and non-T_{FH} cells (**Fig. 2D**). At day 10 post-infection, differentiation of T_{FH} cells, expansion of P14 cells and viral loads in sera and spleens were similar between mice that had received either $Cxcr5^{+/+}$ or $Cxcr5^{-/-}$ P14 cells (**Fig. S6B-D**). Furthermore, the number of non-T_{FH} cells infected with LCMV was similar in the two groups (**Fig. 2E**). In contrast, the frequency of LCMV-infected T_{FH} cells in mice that had received $Cxcr5^{-/-}$ P14 cells was about 2-fold higher than that in mice receiving $Cxcr5^{+/+}$ P14 cells (**Fig. 2E**). In particular, infected T_{FH} cells with high amounts of LCMV (NP[high]) were at least 3-fold more abundant in mice that had received $Cxcr5^{-/-}$ P14 cells compared to mice that had received wildtype P14 cells (**Fig. 2E**). Therefore, the lack of

T_{FC} cells resulted in selective increase of infection in T_{FH} cells, indicating a specific role for CXCR5$^+$ T_{FC} cells in controlling T_{FH} infection.

The anatomical localization of T_{FC} cells suggested that they would also be able to control infected or malignant B cells. To test this idea, we adoptively transferred either *Cxcr5*$^{+/+}$ or *Cxcr5*$^{-/-}$ T_C cells into recipient OT-I mice, which we subsequently infected with MuHV-4 expressing eGFP from an intergenic EF1α promoter to visualize infected cells[22]. At day 9 post-infection, expansion and activation of transferred *Cxcr5*$^{+/+}$ or *Cxcr5*$^{-/-}$ T_C cells was similar (**Fig. S7A, B**). However, the frequency of MuHV-4-infected B cells in mice that had received *Cxcr5*$^{-/-}$ T_C cells was 4.5-fold higher than that in mice that had received *Cxcr5*$^{+/+}$ T_C cells (**Fig. 2F**). Thus, T_{FC} cells contribute to the eradication of virus-infected B cells infection. Consistent with the prominent role of CD8 T cells in controlling nascent B cell lymphoma[23], large numbers of CXCR5$^+$ T_{FC} cells were detected in B cell lymphoma bearing mice (**Fig. S8**). Together, these data demonstrate that T_{FC} cells are phenotypically and functionally specialized effector Tc subset.

To characterize T_{FC} cells comprehensively at the molecular level, we performed transcriptional profiling of CXCR5$^+$ T_{FC} and CXCR5$^-$ non-T_{FC} P14 cells by RNA sequencing at day 8 post-infection. Although both populations shared many molecular characteristics and differed profoundly from their naïve counterparts, we found 1201 transcripts that were significantly up or downregulated (≥ 2-fold, P value < 0.05) in T_{FC} compared to non-T_{FC} cells and make up the T_{FC} transcriptional signature (**Fig. S9 and S10**). T_{FC} cells expressed lower amounts of transcripts encoding effector molecules involved in cytotoxicity, including granzyme A, B, perforin and IFNγ, and exhibited

increased expression of genes involved in memory T cell development, including *Il7r* and *Sell* (encoding CD62L). Furthermore, T_{FC} cells expressed higher amounts of transcripts encoding ICOS, Ly108 and CD200 but lower amounts of that encoding SLAM (**Fig. 3A**). *Havcr2* and *Cd244* (encoding the inhibitory receptors Tim-3 and 2B4) were lower in T_{FC} than in non-T_{FC} cells (**Fig. 3A**), while *Pdcd1* (encoding PD-1) was expressed in similar amounts. Importantly, we confirmed differential expression of many of these molecules at the protein level (**Fig. 3B-E** and **S11A**). Notably, T_{FC} cells did not express ICOSL, a marker for regulatory CD8$^+$ T cells in B cell follicles that were identified in autoimmune diseases[24] (**Fig. S11B**), nor IL-21, the helper cytokine produced by T_{FH} cells to support antibody response[2] (**Fig. S11C**). CXCR5$^+$ T_{FC} P14 cells executed cytotoxic function, although, consistent with their lower expression of some of the cytotoxic molecules, they were less efficient than their CXCR5$^-$ counterparts (**Fig. 3F and S11D**).

While T_{FC} cells expressed similar amounts of *Tbx21* (encoding T-bet) and *Eomesodermin* (*Eomes*) (data not shown), they displayed high expression of the transcriptional regulators *Bcl6*, *Tcf7* (encoding Tcf1) and *Id3*, and low expression of *Prdm1* (encoding Blimp1) and *Id2* (**Fig. 3A, 4A,B** and **S12A,B**). Interestingly, this transcriptional profile was similar to that of Tfh cells[25-32]. Indeed, we found striking enrichment of the transcriptial signature of T_{FC} cells within the gene expression signature associated with T_{FH} cells, with 67.7% of the upregulated genes and 92.2% of the downregulated genes in T_{FC} cells being regulated correspondingly in T_{FH} cells (**Fig. S13A**). Bcl6 plays a key role in T_{FH} biology and is sufficient to drive T_{FH} development[25-27]. Overepression of Bcl6 dramatically increased the expression of CXCR5 on P14 cells

from ~20% to ~60% during LCMV infection (**Fig. 4C**) and resulted in their dramatically increased recruitment to B cell follicles (**Fig. 4D**). Overexpression of Bcl6 was sufficient to recapitulate the T_{FC} phenotype including upregulation of IL-7R, CD62L and ICOS, downregulation of granzyme B and Tim-3, and reduced cyototoxic activity in comparison to control cells (**Fig. S14A-C**). Furthermore, overexpression of Bcl6 enhanced the expression of *Tcf7* and *Id3* but inhibited the expression of *Prdm1* and *Id2* (**Fig. S14D**). Consistent with a critical role for Bcl6 in T_{FC} cell differentiation, Bcl6-deficient P14 cells failed to differentiate into T_{FC} cells (**Fig. 4E**). Therefore, Bcl6 is necessary and sufficient to direct the differentiation of T_{FC} cells. Blimp1 has been shown to antagonize T_{FH} differentiation[25]. In line with an important negative regulatory function for Blimp1 in T_{FC} differentiation, antigen-specific Blimp1-deficient T_C cells showed a marked increase in CXCR5 expression (**Fig. 4F**) and a marked deregulation of T_{FC} transcriptional signature genes (20.2%   upregulated and 25.3% downregulated)[33] (**Fig. S13B**). During T_{FH} development, Tcf1 promotes Bcl6 and inhibits Blimp1 expression[29-31]. In line with a similar role in T_{FC} cells, antigen-specific T_C cells lacking Tcf1 were severely impaired in T_{FC} cell generation (**Fig. 4G**). Id2 and Id3 are transcriptional regulators that sequester E-protein family transcription factors, including E2A, and inhibit CXCR5 expression in thymocytes and peripheral CD4$^+$ T cells[28,32]. Consistent with this notion, loss of Id2 promoted T cell-intrinsic CXCR5 expression (**Fig. 4H**). Similarly, lack of Id3 resulted in enhanced T cell-intrinsic CXCR5 expression in LCMV-specifc Tc cells, whereas overexpression of Id3 in LCMV-specifc Tc cells diminished T_{FC} differentiation (**Fig. 4I, J**). In line with a role for Id proteins in the inhibition of T_{FC} cell generation, Id2 or Id3 deficient T cells[34,35] showed significant deregulation of genes differentially expressed in

T_{FC} cells in comparison to non-T_{FC} cells (**Fig. S13C,D**). Interestingly, while Id3 was expressed predominantly in T_{FC} cells, Id2 was highly expressed in non-T_{FC} cells, suggesting that limiting E protein activity is critical for the coordinate differentiation of both T_{FC} and non-T_{FC} populations.

Consistent with a critical function for Bcl6 in T_{FC} differentiation, we found signficant enrichment of genes bound by Bcl6 among the differentially expressed genes in T_{FC} cells (**Fig. S15A**). However, we did not find evidence for Bcl6 directly regulating the expression of CXCR5 (ref. 36,37). In contrast, chromatin immunoprecipitation followed by deep-sequencing (ChIP-seq) identified two Blimp1- and two E2A binding sites at the *Cxcr5* locus (**Fig. 4K**) that contained the consensus Blimp1- and E2A-binding motifs, respectively (**Fig. S16A**). *In vivo* reporter assays using retroviral vectors[31] (**Fig. S16B**) containing either wildtype or mutated Blimp1 binding motifs (**Fig. S16A**), revealed that Blimp1-mediated suppression of *Cxcr5* promoter activity was abolished when the binding sequence was mutated (**Fig. 4L** and **S16C**). In contrast, E2A-binding promoted the *Cxcr5* promoter-driven transcription; however, this activity was largely abolished in the presence of the adjacent Blimp1 binding site (**Fig. 4M** and **S16D**). We also observed binding of Blimp1 and E2A to *Tcf7*, *Bcl6* and *Id3* as well as binding of E2A at *Id2* (**Fig. S17**), suggesting that both factors play central roles in the transcriptional network regulating T_{FC} development. In line with this notion, we found more than 50% of the genes bound by Blimp1 or E2A were also differentially expressed in T_{FC} cells in comparison to non-T_{FC} cells (**Fig. S15B, C**), suggesting that these two transcription factors broadly regulated T_{FC} cell development. Consistent with an important function for Tcf1, we also found significant enrichment of genes bound by

Tcf1 among the genes differentially expressed in T_{FC} cells (**Fig. S15D**). In conclusion, our data indicate that Bcl6, Blimp1, Tcf1 and E2A (with its regulators Id3 and Id2) form a transcriptional circuit that controls the expression of CXCR5 and directs the differentiation of T_{FC} cells (**Fig. S18**).

Persistence of virus infected cells, in particular T_{FH} cells is one of the major obstacles to eliminating HIV infection in individual on antiretroviral therapy (ART). Studies on HIV-infected humans and monkeys infected with simian immunodeficiency virus (SIV) on ART suggested that insufficient localization of T_C cells to B cell follicles is at least partially responsible for the high level of infection of T_{FH} cells[8,9,11]. Our data show that antigen-specific CD8^{+} T cells can differentiate into a specialized subset of cytotoxic effector cells that gain entry into B cell follicles where they can eliminate infected T_{FH} cells and B cells. T_C entry into the follicles requires up-regulation of Bcl6 and down-modulation of Blimp1, which not only results in expression of CXCR5, but as a trade-off also leads to reduced expression of several cytotoxic effector molecules that require high amount of Blimp1[38,39]. Our results therefore demonstrate that elimination of virus-infected T_{FH} cells or B cells, or cancerous B cells may not only require boosting follicular entry but also cytotoxicity of T_{FC} cells. Understanding how to direct T_{FC} differentiation and function may help to design new strategies for eliminating HIV persistence in T_{FH} cells in HIV-infected individuals on ART, for controlling the infection of B cells with viruses such as by EBV, or for eradicating B cell-derived tumours.

METHODS

Human samples

Lymph nodes (LN) sections for immunofluorescent stains were obtained by inguinal LN resection under local anesthesia, following informed consent with ethical approval at University of Minnesota Institutional Review Board. LN cells for flow cytometry were obtained by fine needle aspiration from HIV-infected subjects, following informed consent with ethical approval at Department of Pathology, Beijing Ditan Hospital, Capital Medical University. Subjects' demographical and clinical characteristics are presented in Table S1. Tonsil specimens were obtained following informed consent with ethical approval from patients undergoing routine tonsillectomy at the Queen Elizabeth Hospital Birmingham via the University of Birmingham Human Biomaterials Resource Centre. Unfractionated mononuclear cells (UMs) were isolated. All patients were confirmed as EBV-positive by qPCR for viral DNA load in total tonsillar UMs[40].

Mice

All mice used in this study were male on C57BL/6J background and were maintained in specific pathogen free animal facilities in Monash University or the Walter and Eliza Hall Institute. For transgenic strains, P14[tg/+] TCR transgenic (specific for LCMV gp_{33-41})[17], SMARTA[tg/+] TCR transgenic (specific for LCMV gp_{61-80})[21], OT-I[tg/tg] TCR transgenic (specific for chicken ovalbumin (OVA)$_{257-264}$), Bcl6[tg/+] transgenic (IµHABcl6, B-cell specific transgene)[23] were described earlier. The gene-deficient mouse strains, Bcl6[Cd4-Cre] (Ref. 41), Prdm1^{fl/fl}-Lck[Cre] (Blimp1[Lck])[38], Id2^{fl/fl}LCK[Cre] (Ref. 42), Id3[gfp/gfp] (GFP knock-in)[28], Tcf7^{fl/fl}-Lck[Cre43], and GFP-reporter strains, Blimp1[+/gfp] (GFP knock-in)[44], Id2[+/gfp35], Id3[+/gfp28] and Il21[+/gfp45] were described earlier. Blimp1-bio:Rosa26[BirA] mice carry a biotin

acceptor sequence at the carboxyl terminus of Blimp1, which was biotinylated *in vivo* by coexpression of the *Escherichia coli* biotin ligase BirA from the *Rosa26*[BirA] allele[46]. Animal experiments were approved by the Animal Ethics Committee of the institutes responsible for housing the mice.

Virus infection

To study the kinetics of CXCR5 expression, cytotoxicity, and follicular entry of CD8^{+} T cells, 6000 purified P14 cells were transferred into congenically marked WT mice. To study the function of T_{FC} cells to control T_{FH} infection, 1000 purified P14 and 1000 SMARTA cells were transferred into OT-I mice. Mice were intravenously (i.v.) injected with LCMV (DOCILE) at 2×10^6 plaque-forming unit (PFU) per mouse one day after adoptive transfer of indicated cells. For the study of MuHV-4 infection, MuHV-4 was engineered to express enhanced GFP (eGFP) under the intergenic eukaryotic promoter EF1α (MuHV4-EF1α-eGFP)[22]. 2×10^7 polyclonal CD8 T cells were transferred into OT-1 mice. One day after adoptive transfer, mice were infected intranasally with 10,000 PFU of MuHV4-eGFP. For the infection with influenza virus, 6000 OT-I cells were transferred into congenically marked WT mice. Mice were i.v. injected with influenza virus strain x-31 (H3N2) expressing OVA at 80 TCID50 per mouse one day later. All recipient mice were 7-12 weeks old at the time of experiments. Spleens were obtained at indicated post-infection time points for analysis. For MuHV-4 infection, mediastinal LNs were obtained for analysis.

Immunization

6000 OT-I cells were transferred into congenically marked WT mice. 50 μg of OVA was emulsified with CFA at 1:1 volume ratio, and 25 μL of the mixture (containing 50 μg of

OVA) were injected into the hock of each mouse. Popliteal lymph nodes were obtained at day 8 after immunization.

Cell lines

C57BL/6-derived MC57 fibrosarcoma cell line was used to titrate virus level in sera and spleens. GP+E-86 (GPE86) is a murine embryonic retrovirus packaging cell line used to produce retroviruses for transduction. Both cells lines were obtained from American Type Culture Collection. Neither cell line is on the list of Cross-Contaminated or Misidentified Cell Lines published by International Cell Line Authentication Committee. Cultures are free of mycoplasma as tested by PlasmoTest™ (Invivogen).

Cell preparation

Cells were prepared by gently mashing spleens or lymph nodes through 70 µm cell strainers. Red blood cells were then lysed with the lysis buffer for 10 minutes on ice. Single cell suspension (SCS) was prepared by gently pipetting the tissues in complete RPMI (cRPMI, consists of 10 mM HEPES, 1X non-essential amino acids solution (Gibco), 1 mM sodium pyruvate, 1X Penicillin-Streptomycin-Glutamate solution (PSG, Gibco), 55 µM 2-mercaptoethanol and 10% FCS in RPMI media).

Generation of chimeric mice

Bone marrow (BM) cells were collected from 7-12 weeks old adult femurs bones by flushing out the tissues within the bones, and SCS were prepared by pipetting the tissues in cRPMI media. BM cells were cryopreserved in liquid nitrogen until further use. Gene-deficient BM cells (CD45.2$^+$) were mixed with WT BM cells (CD45.1$^+$) at 1:1 ratio and transferred into $Rag1^{-/-}$ mice, which had been lethally irradiated twice with 4.875

gray (Gy) of gamma radiation 4 hours apart. BM cells from WT CD45.2[+] BM were also mixed with WT CD45.1[+] BM and reconstituted in recipient mice as control groups. Mice were housed for 6 weeks to allow haematopoietic reconstitution before infection with LCMV DOCILE.

Detection of LCMV DOCILE-infected cells by flow cytometry

Detection of virus-infected cells by flow cytometry was adapted from a previous study[9]. Briefly, hybridoma of rat anti-LCMV nucleoprotein (clone VL4) was cultured in serum-free DMEM media. Culture supernatant was collected and VL4 antibody was purified using protein A (Invitrogen). Purified antibody was labelled with Alexa Flour 647 (AF647, Invitrogen) according to manufacturer's instruction. To reduce the staining background, unconjugated AF647 was removed using ultracentrifugal unit (10 kDa MW cut off, Amicon). Infected splenocytes were stained with Fc-receptor blocking antibody (clone 2.4G2) followed by staining with antibodies against surface markers in FACS buffer for 1 hour at 4°C. Cells were then intracellular permeabilized using Cytofix/Cytoperm (BD, 554722) for 30 minutes on ice. AF647-VL4 was incubated with the cells for 30 minutes at room temperature (RT). Splenocytes from uninfected mice were used as negative control.

qPCR for quantification of viral and gene expression

Quantification of DOCILE RNA was performed by a quantitative PCR (qPCR) method adapted from a previous study[10]. Briefly, splenocytes were pooled from eight LCMV (DOCILE)-infected mice collected on day 15 p.i. and stained with surface antibodies and different subsets of CD4^{+} T cells were purified by flow cytometry. RNA was isolated from sorted cells using the RNAeasy Mini Kit (Qiagen). RNA of LCMV GP and a house

keeping gene β-actin was reverse-transcribed using 2 pmol of LCMV GP (GCAACTGCTGTGTTCCCGAAAC) and mouse β-actin (GAGGTAGTCTGTCAGGTCCC) reverse primers and Superscript III Reversed Transcriptase kit (Invitrogen) according to manufacturer's instruction. Complementary DNA were then quantified using the Accupower Q-PCR kit (Bioneer) and the same LCMV GP or mouse β-actin reverse primers, with the addition of forward primers for GP (CATTCACCTGGACTTTGTCAGACTC) and β-actin (CCAACCGTGAAAAGATGACC). For quantification of gene transcripts, Bioneer RT cycler kit were used to synthesis total cDNA as per manufacturer's instruction. cDNA were quantified using qPCR kit as above with the following primers: *Prdm1* forward 5' CTTGTGTGGTATTGTCGGGAC 3' and reverse 5' CACGCTGTACTCTCTCTTGG 3'; *Id2* forward 5' ATCCTGTCCTTGCAGGCATC 3' and reverse 5' TCTCCTGGTGAAATGGCTGA 3'; *Id3* forward 5' CATCTCCCGATCCAGACAGC 3' and reverse 5' GAAGCTCATCCATGCCCTCA 3'; *Tcf7* forward 5' CTATCCCAGGTTCACCCACC 3', and reverse 5' TTCTCTGCCTTGGGTTCTGC 3'. Relative fold change was calculated by $2^{-(\Delta CT \text{ experiment} - \Delta CT \text{ control})}$. $\Delta CT = CT^{\text{gene of interest}} - CT^{\beta\text{-actin}}$.

Virus titration in serum and spleen

Virus titration was adapted from a previous study[47]. Briefly, the MC57 murine fibroblast cell line was incubated with virus-containing samples to infect MC57 cells for 24 hours in complete DMEM (cDMEM, containing 10% FCS and 1X PSG in DMEM media). Cells were then washed with DPBS, trypsinized and washed with FACS buffer. Intracellular staining with AF647-VL4 was performed on the infected MC57 as described above. Infected MC57 were identified as VL4$^+$ cells. A standard curve was generated using a

stock of virus with known PFU concentration (as measured by standard plaque forming assay). Viral PFU in tested samples were extrapolated using the standard curve. To ensure that values fell within the linear range of the standard curve, sera were diluted at 1:100 and spleens were weighed and homogenized at 100 μg/ml.

Flow cytometry

Cells were stained with Fc-receptor blocking antibodies (clone 2.4G2) for 10 minutes on ice to block non-specific staining. Primary anti-mouse antibodies were then added and incubated for 1 hour at 4°C, followed by 30 minutes of streptavidin or secondary antibody staining on ice. Primary anti-human antibodies were incubated for 30 minutes at room temperature. Staining for CCR7 was done at 37°C for 20 minutes. For staining of intracellular cytokines, whole splenocytes were stimulated with 5 μg/mL of gp33 peptide in the presence of monensin and brefeldin A (eBioscience, 00-4506 and 00-4505) for 4 hours at 37°C. Stimulated cells were then subject to the same antibody-staining protocol as above.

For intracellular staining, cells were washed twice after surface staining and permeabilized using Cytofix/Cytoperm (BD, 554722) for 30 minutes on ice. Antibodies specific for intracellular proteins were diluted in Perm/Wash Buffer (BD, 554723) and incubated for 30 minutes at RT. For intranuclear staining, cells were permeabilized using Transcription Factor Staining Buffer Set (eBioscience, 00-5523-00) for 30 minutes on ice. Antibodies specific for intranuclear proteins were diluted in Permeabilization Buffer (eBioscience, 00-8333) and incubated for 60 minutes at RT.

The following anti-mouse antibodies used for staining were purchased from Biolegend unless otherwise indicated: Biotin-CXCR5 (clone L138D7), AF488-SLAM (clone TC15-

12F12.2), PE-Bcl6 (clone K112-91, BD), PE-Perforin (clone eBioOMAK-D, eBioscience), PE-Tim-3 (clone B8.2C12), PECy7-IFNγ (clone XMG1.2, BD), PECy7-Thy1.1 (BD XX) PE-CD200 (clone OX-90), PECy7-ICOS (clone C398.4A), PECy7-2B4 (clone m2B4(B6)458.1), APC-Granzyme A (clone GzA-3G8.5, eBioscience), APC-Ly108 (clone 330-AJ), APC-H-2D^b-GP^{33}-tetramer (MBL), APCCy7-CD45.1 (clone A20), AF700-CD8 (clone 53-6.7), BV421-PD1 (clone J43, BD), Pacific Blue-Granzyme B (clone GB11), BV510-CD44 (clone IM7, BD), BV421-CCR7 (clone 4B12), BV605-IL-7R (clone A7R34), BV605-CD4 (clone RM4-5), BV711-CD62L (clone MEL-14), BUV737-TCRβ (clone H57-59, BD), BUV395-B220 (clone RA3-6B2, BD), Streptavidin-PECy-5.5 (ThermoFisher Scientific). Antibodies of the same or overlapping fluorophores were stained separately. T_C and T_H cells were gated on CD8$^+$TCRβ$^+$B220$^-$ and CD4$^+$TCRβ$^+$B220$^-$, respectively, for FACS analysis. To exclude dead cells, cells were stained with 7-AAD. To exclude dead cells from staining protocols that involved permeabilization, cells were stained with Zombie Aqua™ Fixable Viability Kit (Biolegend) before permeabilization.

For staining of LN from HIV-infected patients, the following antibodies are used: FITC-TCRαβ (clone IP26, Biolegend), PECy7-CCR7 (clone G043H7, BD), AF647-CXCR5 (clone RF8B2, BD), APCCy7-CD45RA (clone HI100, BD), BV510-CD8a (clone RPA-T8, BD), BV786-CD19 (clone HIB19, BD). Antibodies of the same or overlapping fluorophores were stained separately. T_C cells were gated on CD8$^+$TCRαβ$^+$CD19$^-$ for FACS analysis. To exclude dead cells, cells were stained with 7-AAD.

For the staining of EBV specific tonsillar CD8 T cells, according to their HLA class I type, tonsillar UMs were exposed for 30mins at 37°C to either HLA-A*0201 tetramers

carrying YVLDHLIVV (YVL) or GLCTLVAML (GLC) peptides (derived from EBV antigens BRLF1 and BMLF1 respectively), or HLA-B*0801 tetramer carrying RAKFKQLL (RAK) peptide (BZLF1), as previously described [48]. All tetramers were APC-conjugated. Cells were subsequently washed and stained with live/dead fixable violet cell stain kit (Invitrogen) for 20 mins at RT. Following a further wash, cells were stained with the following antibodies for 30 minutes at RT: CD4 ECD (clone SFCI12T4D11, Beckman Coulter), CD8 Brilliant Violet 510 (clone SK1, Biolegend), CD14 Pacific Blue (clone HCD14, Biolegend), CD19 Pacific Blue (clone HIB19, Biolegend), CXCR5 PE-Cy7 (clone J252D4, Biolegend), CD45RA Alexa Fluor 700 (clone HI100, Biolegend), CCR7 FITC (clone 150503, R&D Systems).

All samples were subsequently analyzed using BD LSR II flow cytometer. Validation profile and citation for each antibody can be found on 1DegreeBio website.

Immunofluorescence

Immunofluorescence analysis was performed either alone or after RNAscope in situ hybridization as previously described[11,27,49]. For mouse spleen tissues, middle section of spleens were cut and submerged in optimal cutting temperature (OCT) compound and stored at -80°C. Human LNs were processed in similar fashion. OCT block were then sectioned at 6-7μm thickness and fixed with acetone for 10 minutes at -20°C. Sections were blocked with Fc-receptor blocking antibody (clone 2.4G2) followed by staining with primary antibodies and secondary antibodies. All steps were performed at RT for 60 minutes in the dark. Slides were washed and incubated with 0.1% Sudan Black B in 70% ethanol (Cat. No.4410; ENG Scientific) followed by TBS for 30 minutes at room temperature to quench autofluorescence. Sections were counterstained with DAPI and

mounted using Fluoromount G™ (ProSciTech) or Prolong® Gold (Invitrogen). Mouse sections were visualized using an Olympus Provis AX70 Widefield fluorescence microscope. Human LN sections were visualized using Olympus FV10i confocal microscope using a 60x phase contrast oil-immersion objective (NA 1.35) imaging. Quantification of Tc was performed by visually counting cells per area of section. Follicular/Non-Follicular ratio was calculated by dividing number of follicular by non-follicular P14.

The following anti-mouse antibodies were used for immunofluorescence: Biotin-CD3 (clone 145-2C11, Biolegend), Biotin-CD4 (clone H129.19, BD), AF647-B220 (clone RA3-6B2, Biolegend), AF647-CD45.1 (clone A20, Biolegend), AF488-CD8 (clone 53-6.7, Biolegend) and AF555-streptavidin (ThermoFisher Scientific). Following anti-human antibodies were used: rabbit monoclonal anti-CD8 (clone SP16, Thermofisher) and mouse monoclonal anti-CD20 (clone L26, Dako) with AF488 or AF594-donkey anti-rabbit, and AF488 or AF647-donkey anti-mouse (Invitrogen). Validation profile and citation for each antibody can be found on 1DegreeBio website.

Retroviral vector-mediated gene overexpression

GFP bicistronic retroviral vector containing Bcl6 has been described[25]. mCherry bicistronic retroviral vector containing Id3 was generated by cloning Id3 into the vector. Thy1.1 reporter constructs (Fig S15B) were kindly provided by Lilin Ye[29]. Cloning of cassettes were performed as previously described[29]. Retroviruses were then generated by transfecting the plasmids into a retrovirus-packaging cell line GPE86. GFP or mCherry positive GPE86 were sorted to isolate stably transfected cells. Stably transfected GPE86 were then cultured in cDMEM for 48 hours and retrovirus in the

culture supernatant were collected for the transduction of primary CD8$^+$ T cells. To prepare primary CD8$^+$ T cells for transduction, naïve CD8$^+$ T cells were purified from P14 mice and stimulated with plate-bound anti-CD3 and anti-CD28 for 48 hours. For the transduction, cells were spinoculated at 800 g for 1 hour at 32°C. Cells were rested in fresh cRPMI media containing 20 ng/mL of rmIL7. After 48 hours, GFP$^+$ or mCherry$^+$ P14 were sorted and 6000 sorted cells were transferred into congenically marked WT mouse. 24 hours later, mice were infected with LCMV (DOCILE). For the study of Bcl6 overexpression on transcriptional regulation of other genes, cells were rested in 10 ng/mL of IL-2 and 100 ng/mL of IL-12 for 48 hours, GFP$^+$ cells were then sorted and subjected to Q-PCR analysis as described above.

Ex vivo cytotoxic assay

The *ex vivo* cytotoxic assay was adapted from a previous study[50]. Briefly, CD44$^-$ CD62L$^+$CXCR5$^-$ (Naïve) P14 cells were sorted from P14 mice and transferred into congenically marked WT host, followed by infection with Docile. 8 days after infection, splenocytes were isolated and sorted for CD44$^+$CD62L$^-$CXCR5$^-$ (CXCR5$^-$ non-T$_{FC}$) and CD44$^+$CD62L$^-$CXCR5$^+$ (CXCR5$^+$ T$_{FC}$) P14 cells. These cells were used as effector cells (E). To prepare target cells, splenocytes were isolated from uninfected WT mice and stained with 20 µM or 1 µM of cell trace violet (CTV) dye (Invitrogen). 20 µM-stained (CTV^{hi}) splenocytes were incubated with gp^{33} peptide (KAVYNFATM) at 10 µg/mL for 1 hour at 37°C in cRPMI media. 1 µM-stained splenocytes (CTV^{lo}) were incubated with cRPMI media alone. Cells were then washed extensively, counted, mixed at 1:1 ratio and used as target cells (T). To prepare T$_{FH}$ and non-T$_{FH}$ target cells, SMARTA cells were injected into congenic WT mice and infected with DOCILE. D8 p.i., *in vivo*

differentiated TFH and non-TFH SMARTA cells were sorted and stain with CTV as above. Effector cells and target cells were then mixed at 4:1 E:T ratio in U-bottom 96-well and cultured for 10 hours in cRPMI at 37°C. Cells were then stained with 7-AAD to exclude dead cells and analyzed with flow cytometry. % specific cytotoxicity was calculated as follows:

Effector cytotoxicity (A) = (%CTV^{hi}/%CTV^{lo})

Target only cytotoxicity (B) = (%CTV^{hi}/%CTV^{lo})

% specific cytotoxicity = (1-A/B)×100

For *ex vivo* cytotoxicity of Bcl6-overexpressed P14 cells, transduced cells were re-stimulated with plate-bound anti-CD3/CD28 for 24 hours. GFP$^+$ cells were sorted and used as effector cells in the *ex vivo* cytotoxicity assay as described above.

RNA sequencing

CD44$^-$CD62L$^+$CXCR5$^-$ naïve CD8$^+$ T cells were purified from P14 mice and transferred into congenically marked WT mice. RNA was also extracted from purified naïve P14 cells. 24 hours after adoptive transfer, mice were then infected with LCMV (DOCILE). 8 days p.i., splenocytes were collected and sorted for CD44$^+$CXCR5$^-$ (CXCR5$^-$ non-T$_{FC}$) and CD44$^+$CXCR5$^+$ (CXCR5$^+$ T$_{FC}$) P14 cells, followed by RNA extraction using the RNAeasy Micro Kit (Qiagen). RNA integrity was analyzed using Agilent RNA 6000 Nano Kit (Agilent). PolyA-enrichment was used for library preparation and 50 bp one-end sequencing was performed by Monash Health Translation Precinct Medical Genomics Facility.

For the transcriptional profiling of Blimp1-deficient CD8 T cells, we generated mixed bone marrow chimeric mice of Blimp1^{LCK} as described above. These mice were rested for 6-9 weeks and first inoculated i.p. with 10^7 PFU of influenza virus A/PR/8/34, followed by secondary infection with the x31 4-6 weeks later. 9 days after x31 infection, mediastinal LN were obtained, and antigen-specific CD8$^+$ T cells were sorted using MHC class I (H-2D^b) tetramers complexed with influenza NP$_{366-374}$ (NP$_{366}$) peptide. RNA isolation and sequencing were then performed as above.

Bio-ChIP sequencing

Blimp1$^{Bio/Bio}$ and *Tcf3*$^{Bio/Bio}$ mice carry a biotin acceptor sequence at the carboxyl terminus of Blimp1 and E2A (*Tcf3*), which can be biotinylated *in vivo* by coexpression of the *Escherichia coli* biotin ligase BirA from the *Rosa26*^{BirA} allele. Blimp1 Bio-ChIP-seq was performed with splenic CD8$^+$ T cells from *Blimp1*$^{Bio/Bio}$ *Rosa26*$^{BirA/BirA}$ mice that were stimulated first with anti-CD3, anti-CD28 and IL-2 (100 U/ml) for 3 days and then with IL-2 and IL-12 (5 ng/ml) for another 2 days. Chromatin from ~3 x 10^8 CD8$^+$ T cells was prepared using a lysis buffer containing 0.25% SDS prior to chromatin precipitation by streptavidin pulldown (Bio-ChIP), as described[46]. The precipitated genomic DNA was quantified by real-time PCR. E2A Bio-ChIP-seq was performed with total thymocytes from *Tcf3*$^{Bio/Bio}$ *Rosa26*$^{BirA/BirA}$ mice. The precipitated genomic DNA was amplified with the KAPA Real Time Amplification kit (KAPA Biosystems). Cluster generation and sequencing was carried out using the Illumina HiSeq 2000 system with a read length of 50 nucleotides according to the manufacturer's guidelines.

To analyze ChIP-seq data, Bowtie2.2.8 has been used for alignment with mouse mm9 as reference genome, MACS2.1.0 for peak calling with p value $10e^{-10}$ as cutoff.

The peak table with the peak starting and ending location was mapped to genes with the following strategies: Peaks were assigned to genes in a stepwise manner by prioritizing genes containing peaks in their promoter and/or gene body. For this, peaks with -2.5 kb to TSS and +2.5 kb to TES were first assigned to the corresponding gene. Other peaks within 50kb to gene body were assigned to the nearest gene for long distance regulation. R functions Venn in g-plots package and barcode plots in limma package were used to generate the figures. Bcl6 ChIP-seq (GSM1857225)[37], E2A ChIP-seq (to be deposited to the GEO repository) and Tcf1 ChIP-seq (GSM1889262)[51] were obtained from published data.

Bioinformatics analysis of RNA sequencing and ChIP-seq data

To analyze RNA sequencing data, RPKM (Read per kilobase per million) were obtained from raw dataset and $\log_2$ transformed after replacing zero by the minimum value in the dataset. The $\log_2$ RPKM data were quantile normalized. The R statistical software (version 3.1.2) was used to calculate differentially expressed genes between naïve, $CXCR5^+$ $T_{FC,}$ and $CXCR5^-$ non-T_{FC} cells. Genes satisfying the following criteria were chosen for analysis: first, the average count is more than 100 in at least one sample group and second, the global false discovery rate (FDR) is controlled at 0.05 with a minimum fold-change of 2. This generated a "T_{FC} versus non-T_{FC} signature gene set". The same method was used to generate the "Blimp1 KO versus Blimp1 WT gene set". RNA sequencing results can be accessed under GSE68056. The same methods were used to generate T_{FH} vs non-T_{FH} cells signature gene set (GSE16697)[25], Id2 KO vs WT gene set (GSE44140)[35], Id3 KO vs WT gene set (GSE23568)[34] from previously published data.

For the enrichment analysis, rotation gene set test (ROAST) of the signature gene set between each dataset was compared, providing the directional p-values and the percentage of the commonly regulated genes in the barcode plots.

Statistical analysis

Preliminary experiments were performed using 3-5 mice to determine the expected means and sample distributions of the control and experimental groups. The means and sample distributions were then used to calculate the sample size required to test the hypothesis in subsequent experiments using MedCalc (exact numbers of samples were indicated in figure legend). As normality of the sample distributions cannot be tested with small sample sizes ($n \leq 5$), non-parametric two-sided Mann-Whitney's U-tests were performed for comparison between two groups without assumption of normal distribution. One-way ANOVA was used to calculate univariate data set with more than two groups. Two-way ANOVA was used to calculate multivariate data set. Wilcoxon matched-pairs rank test was to calculate paired samples between two groups. Repeated-measure (RM) two-way ANOVA was used to calculate paired multivariate samples. Animals were of matched sex and age, no randomisation were performed for the grouping of animals. Blinding was not performed due to the objective measurement of the experimental data. All statistical analysis were performed using Prism GraphPad.

REFERENCES

1   Mueller, S. N., Gebhardt, T., Carbone, F. R. & Heath, W. R. Memory T cell subsets, migration patterns, and tissue residence. *Annual review of immunology* **31**, 137-161, doi:10.1146/annurev-immunol-032712-095954 (2013).

2   Vinuesa, C. G., Linterman, M. A., Yu, D. & MacLennan, I. C. Follicular Helper T Cells. *Annual review of immunology* **34**, 335-368, doi:10.1146/annurev-immunol-041015-055605 (2016).

3   Barton, E., Mandal, P. & Speck, S. H. Pathogenesis and host control of gammaherpesviruses: lessons from the mouse. *Annual review of immunology* **29**, 351-397, doi:10.1146/annurev-immunol-072710-081639 (2011).

4   Lindqvist, M. *et al.* Expansion of HIV-specific T follicular helper cells in chronic HIV infection. *The Journal of clinical investigation* **122**, 3271-3280, doi:10.1172/jci64314 (2012).

5   Petrovas, C. *et al.* CD4 T follicular helper cell dynamics during SIV infection. *The Journal of clinical investigation* **122**, 3281-3294, doi:10.1172/jci63039 (2012).

6   Perreau, M. *et al.* Follicular helper T cells serve as the major CD4 T cell compartment for HIV-1 infection, replication, and production. *The Journal of experimental medicine* **210**, 143-156, doi:10.1084/jem.20121932 (2013).

7   Pissani, F. & Streeck, H. Emerging concepts on T follicular helper cell dynamics in HIV infection. *Trends in immunology* **35**, 278-286, doi:10.1016/j.it.2014.02.010 (2014).

8   Banga, R. *et al.* PD-1 and follicular helper T cells are responsible for persistent HIV-1 transcription in treated aviremic individuals. *Nature medicine*, doi:10.1038/nm.4113 (2016).

9   Hong, J. J., Amancha, P. K., Rogers, K., Ansari, A. A. & Villinger, F. Spatial alterations between CD4(+) T follicular helper, B, and CD8(+) T cells during simian immunodeficiency virus infection: T/B cell homeostasis, activation, and potential mechanism for viral escape. *Journal of immunology* **188**, 3247-3256, doi:10.4049/jimmunol.1103138 (2012).

10   Vinuesa, C. G. HIV and T follicular helper cells: a dangerous relationship. *The Journal of clinical investigation* **122**, 3059-3062, doi:10.1172/JCI65175 (2012).

11   Fukazawa, Y. *et al.* B cell follicle sanctuary permits persistent productive simian immunodeficiency virus infection in elite controllers. *Nature medicine* **21**, 132-139, doi:10.1038/nm.3781 (2015).

12   Kaech, S. M. & Cui, W. Transcriptional control of effector and memory CD8+ T cell differentiation. *Nature reviews. Immunology* **12**, 749-761, doi:10.1038/nri3307 (2012).

13   Chang, J. T., Wherry, E. J. & Goldrath, A. W. Molecular regulation of effector and memory T cell differentiation. *Nature immunology* **15**, 1104-1115, doi:10.1038/ni.3031 (2014).

14   Quigley, M. F., Gonzalez, V. D., Granath, A., Andersson, J. & Sandberg, J. K. CXCR5+ CCR7- CD8 T cells are early effector memory cells that infiltrate tonsil B cell follicles. *European journal of immunology* **37**, 3352-3362, doi:10.1002/eji.200636746 (2007).

15   Vinuesa, C. G. & Cyster, J. G. How T cells earn the follicular rite of passage. *Immunity* **35**, 671-680, doi:10.1016/j.immuni.2011.11.001 (2011).

16   Zhou, X., Ramachandran, S., Mann, M. & Popkin, D. L. Role of lymphocytic choriomeningitis virus (LCMV) in understanding viral immunology: past, present and future. *Viruses* **4**, 2650-2669, doi:10.3390/v4112650 (2012).

17   Kyburz, D. *et al.* T cell immunity after a viral infection versus T cell tolerance induced by soluble viral peptides. *European journal of immunology* **23**, 1956-1962, doi:10.1002/eji.1830230834 (1993).

18   Hogquist, K. A. *et al.* T cell receptor antagonist peptides induce positive selection. *Cell* **76**, 17-27 (1994).

19   Homann, D., McGavern, D. B. & Oldstone, M. B. Visualizing the viral burden: phenotypic and functional alterations of T cells and APCs during persistent infection. *Journal of immunology* **172**, 6239-6250 (2004).

20   Baca Jones, C. *et al.* Direct infection of dendritic cells during chronic viral infection suppresses antiviral T cell proliferation and induces IL-10 expression in CD4 T cells. *PloS one* **9**, e90855, doi:10.1371/journal.pone.0090855 (2014).

21   Oxenius, A., Bachmann, M. F., Zinkernagel, R. M. & Hengartner, H. Virus-specific MHC-class II-restricted TCR-transgenic mice: effects on humoral and cellular immune responses after viral infection. *European journal of immunology* **28**, 390-400 (1998).

22   Gaspar, M. *et al.* Murid herpesvirus-4 exploits dendritic cells to infect B cells. *PLoS Pathog* **7**, e1002346, doi:10.1371/journal.ppat.1002346 (2011).

23   Afshar-Sterle, S. *et al.* Fas ligand-mediated immune surveillance by T cells is essential for the control of spontaneous B cell lymphomas. *Nature medicine* **20**, 283-290, doi:10.1038/nm.3442 (2014).

24   Kim, H. J., Verbinnen, B., Tang, X., Lu, L. & Cantor, H. Inhibition of follicular T-helper cells by CD8(+) regulatory T cells is essential for self tolerance. *Nature* **467**, 328-332, doi:10.1038/nature09370 (2010).

25   Johnston, R. J. *et al.* Bcl6 and Blimp-1 are reciprocal and antagonistic regulators of T follicular helper cell differentiation. *Science* **325**, 1006-1010, doi:10.1126/science.1175870 (2009).

26   Nurieva, R. I. *et al.* Bcl6 mediates the development of T follicular helper cells. *Science* **325**, 1001-1005, doi:10.1126/science.1176676 (2009).

27   Yu, D. *et al.* The transcriptional repressor Bcl-6 directs T follicular helper cell lineage commitment. *Immunity* **31**, 457-468, doi:10.1016/j.immuni.2009.07.002 (2009).

28   Miyazaki, M. *et al.* The opposing roles of the transcription factor E2A and its antagonist Id3 that orchestrate and enforce the naive fate of T cells. *Nature immunology* **12**, 992-1001, doi:10.1038/ni.2086 (2011).

29   Choi, Y. S. *et al.* LEF-1 and TCF-1 orchestrate T(FH) differentiation by regulating differentiation circuits upstream of the transcriptional repressor Bcl6. *Nature immunology* **16**, 980-990, doi:10.1038/ni.3226 (2015).

30   Wu, T. *et al.* TCF1 Is Required for the T Follicular Helper Cell Response to Viral Infection. *Cell reports* **12**, 2099-2110, doi:10.1016/j.celrep.2015.08.049 (2015).

31   Xu, L. *et al.* The transcription factor TCF-1 initiates the differentiation of T(FH) cells during acute viral infection. *Nature immunology* **16**, 991-999, doi:10.1038/ni.3229 (2015).

32   Shaw, A. L. *et al.* Id2 reinforces TH1 differentiation and inhibits E2A to repress TFH differentiation. *Nature immunology* (2016).

33   Xin, A. e. a. A combinatorial threshold model for effector differentiation of CD8+ T cells mediated by Blimp-1 and T-bet. *Nature immunology* **In press** (2016).

34   Ji, Y. *et al.* Repression of the DNA-binding inhibitor Id3 by Blimp-1 limits the formation of memory CD8+ T cells. *Nature immunology* **12**, 1230-1237, doi:10.1038/ni.2153 (2011).

35   Masson, F. *et al.* Id2-mediated inhibition of E2A represses memory CD8+ T cell differentiation. *Journal of immunology* **190**, 4585-4594, doi:10.4049/jimmunol.1300099 (2013).

36   Hatzi, K. *et al.* BCL6 orchestrates Tfh cell differentiation via multiple distinct mechanisms. *J Exp Med* **212**, 539-553, doi:10.1084/jem.20141380 (2015).

37   Liu, X. *et al.* Genome-wide Analysis Identifies Bcl6-Controlled Regulatory Networks during T Follicular Helper Cell Differentiation. *Cell reports* **14**, 1735-1747, doi:10.1016/j.celrep.2016.01.038 (2016).

38   Kallies, A., Xin, A., Belz, G. T. & Nutt, S. L. Blimp-1 transcription factor is required for the differentiation of effector CD8(+) T cells and memory responses. *Immunity* **31**, 283-295, doi:10.1016/j.immuni.2009.06.021 (2009).

39   Rutishauser, R. L. *et al.* Transcriptional repressor Blimp-1 promotes CD8(+) T cell terminal differentiation and represses the acquisition of central memory T cell properties. *Immunity* **31**, 296-308, doi:10.1016/j.immuni.2009.05.014 (2009).

40   Junying, J. *et al.* Absence of Epstein-Barr virus DNA in the tumor cells of European hepatocellular carcinoma. *Virology* **306**, 236-243 (2003).

41   Hollister, K. *et al.* Insights into the role of Bcl6 in follicular Th cells using a new conditional mutant mouse model. *Journal of immunology* **191**, 3705-3711, doi:10.4049/jimmunol.1300378 (2013).

42   Jackson, J. T. *et al.* Id2 expression delineates differential checkpoints in the genetic program of CD8alpha+ and CD103+ dendritic cell lineages. *EMBO J* **30**, 2690-2704, doi:10.1038/emboj.2011.163 (2011).

43   Steinke, F. C. *et al.* TCF-1 and LEF-1 act upstream of Th-POK to promote the CD4(+) T cell fate and interact with Runx3 to silence Cd4 in CD8(+) T cells. *Nature immunology* **15**, 646-656, doi:10.1038/ni.2897 (2014).

44   Kallies, A. *et al.* Plasma cell ontogeny defined by quantitative changes in blimp-1 expression. *J Exp Med* **200**, 967-977, doi:10.1084/jem.20040973 (2004).

45   Luthje, K. *et al.* The development and fate of follicular helper T cells defined by an IL-21 reporter mouse. *Nature immunology* **13**, 491-498, doi:10.1038/ni.2261 (2012).

46   Minnich, M. *et al.* Multifunctional role of the transcription factor Blimp-1 in coordinating plasma cell differentiation. *Nature immunology* **17**, 331-343, doi:10.1038/ni.3349 (2016).

47   Korns Johnson, D. & Homann, D. Accelerated and improved quantification of lymphocytic choriomeningitis virus (LCMV) titers by flow cytometry. *PloS one* **7**, e37337, doi:10.1371/journal.pone.0037337 (2012).

48   Hislop, A. D., Annels, N. E., Gudgeon, N. H., Leese, A. M. & Rickinson, A. B. Epitope-specific evolution of human CD8(+) T cell responses from primary to

persistent phases of Epstein-Barr virus infection. *J Exp Med* **195**, 893-905 (2002).

49   Deleage, C. *et al.* Defining HIV and SIV Reservoirs in Lymphoid Tissues. *Pathog and Immun* **1**, 39, doi:10.20411/pai.v1i1.100 (2016).

50   Jedema, I., van der Werff, N. M., Barge, R. M., Willemze, R. & Falkenburg, J. H. New CFSE-based assay to determine susceptibility to lysis by cytotoxic T cells of leukemic precursor cells within a heterogeneous target cell population. *Blood* **103**, 2677-2682, doi:10.1182/blood-2003-06-2070 (2004).

51   Xing, S. *et al.* Tcf1 and Lef1 transcription factors establish CD8(+) T cell identity through intrinsic HDAC activity. *Nature immunology* **17**, 695-703, doi:10.1038/ni.3456 (2016).

AUHTOR CONTRIBUTIONS

Y.A.L. planned and performed most experiments with the support from Y.C. and H.S.O.; Y.C. and A.A. performed experiments related to retrovirus-mediated gene overexpression; D.W. and J.X. performed bioinformatics analysis; K.M. performed experiments to generate chimeric mice; C.D, J.G.C., G.J.B., T.W.S. and J.D.E. performed immunofluorescent staining and quantification of HIV samples; M.M., M.B. and A.K. did or analyzed the ChIP sequencing experiments; B.J.M., H.M.L. and U.P. performed analysis of EBV samples; Y.W. Z.H., L.S., P.W., and Y.T. performed flow cytometry on HIV samples; K.A.F., I.C. and S.R.M. performed the experiment of influenza infection; J.G.T., C.C.A. and M.P. provided support for experiments of LCMV and relevant models; H.K.L. provided support for experiment to quantify viral RNA; A.L.D. provided Bcl6$^{fl/fl}$ mice. G.T.B. provided support on MuHV-4 model; A.L.L. and S.R.L. contributed to the scientific planning; D.Y. and A.K. oversaw and designed the study; Y.A.L. and D.Y. analyzed data; D.Y., Y.A.L. and A.K. wrote the manuscript.

LEGENDS

Figure 1: CXCR5 mediates the follicular entry of T_C cells. (A) Immunofluorescent (IF) staining of B cells (anti-CD20, green), $CD8^+$ T cells (anti-CD8, red), and nuclei (DAPI, blue) of lymph node (LN) sections from HIV-uninfected (HIV-) or HIV-infected (HIV+) individuals. The number of $CD8^+$ T cells in B cell follicle (F) and T cell zone (T) were calculated from 7 uninfected and 15 HIV-infected individuals, respectively. **(B)** IF staining of HIV-RNA (red), $CD8^+$ T cells (green) and B cells (blue) of LN section from an HIV-infected individual. Higher magnification of the B cell follicle is shown in yellow box insets, scale bar = 100µm (A, B). **(C)** Flow cytometry (FACS) analysis of CXCR5 expression on naïve ($CCR7^+CD45RA^+$) or effector ($CCR7^-CD45RA^-$) T_C in LN from HIV-infected individuals. Each symbol represents naïve or effector populations from four individuals. **(D-F)** Congenically marked ($CD45.1^+$) P14 cells were adoptively transferred into wildtype (WT) ($CD45.2^+$) mice, which were then infected with LCMV (DOCILE). **(D)** IF staining of B cells (anti-B220, red) and P14 cells (anti-CD45.1, green) in splenic sections collected at indicated time points post-infection (p.i.). **(E)** FACS analysis of CXCR5 expression on P14 cells or on endogenous gp_{33}-H-$2D^b$ tetramer$^+$ T_C cells (from WT mice without P14 cells) at day 8 (D8) p.i. **(F)** CXCR5 expression on P14 cells at indicated time points p.i. **(G)** $CD45.2^+$ WT mice that had received $Cxcr5^{+/+}$ or $Cxcr5^{-/-}$ P14 cells were infected with LCMV (DOCILE). IF staining of splenic sections show the localization of P14 cells at day 15 p.i. The number of P14 cells in B cell follicle and T cell zone were calculated from 8 independent sections of 4 mice for each group. **(H)** FACS analysis of CXCR5 expression on polyclonal T_C cells in the mediastinal LN of uninfected or MuHV4-infected mice (D8 p.i.). **(I)** FACS analysis of tonsil cells from healthy EBV-

carriers shows the CXCR5 expression on naïve or tetramer[+] (Tet+) T_C cells. Each symbol represents naïve or tetramer[+] T_C from two healthy carriers with HLA-A*0201 (YVL and GLC peptides) and one with HLA-B*0801 (RAK peptide) haplotypes. Data are representative of two (D-F, H) or three (G) independent experiments. Each symbol represents the value of an independent section (A, G) or one mouse (F, H); bars represent means. *$P < 0.05$, **$P < 0.01$, as calculated by Wilcoxon matched-pairs signed rank test (C, I), one-way ANOVA (F, H) or two-way ANOVA (A, G) followed by Sidak's multiple comparison test.

Figure 2: T_{FC} cells specifically control infection in B cell follicles. (A-C) Mice were infected with LCMV (DOCILE). IF staining of a spleen section representative of 5 mice showing the infection of T_H cells (B220, green, CD4, red and LCMV, blue) in B cell follicle (upper right) and T cell zone (lower right) at D15 p.i. (A). Infection in T_H subsets (gated as in B) was measured by intracellular staining with anti-LCMV nucleoprotein (NP) antibody (VL4) at indicated time points (C). **(D-E)** OT-I mice that had received P14 and SMARTA cells were infected with LCMV (DOCILE). Gating of T_{FH} and non-T_{FH} subsets (D) was shown together with infection of T_{FH} (E, top) and non-T_{FH} (E, bottom) subsets from SMARTA cells. Graphs show the infection level of each subset (E, right panel). **(F)** OT-I mice that had received polyclonal Tc were infected with MuHV4-EF1α-eGFP. Infected B cells were measured by GFP expression on B220^{+} cells by FACS at D9 p.i.. Each symbol represents one mouse; bars represent means. Data are representative of two independent experiments. *$P < 0.05$, **$P < 0.01$, as calculated by

Mann-Whitney's U-test (F), one-way ANOVA (C) or two-way ANOVA (E) followed by Sidak's multiple comparison tests.

Figure 3: CXCR5$^+$ T$_{FC}$ cells have a distinct transcriptional profile and phenotype. Congenically marked (CD45.1$^+$) P14 cells were adoptively transferred into WT (CD45.2$^+$) mice, which were then infected with LCMV (DOCILE). **(A)** At D8 p.i., CXCR5$^+$ T$_{FC}$ and CXCR5$^-$ non-T$_{FC}$ P14 cells sorted from three infected mice were subjected to RNA-Seq. Depicted in black are the 650 and 551 genes found to be significantly (P value < 0.05, fold changes ≥ 2) up-regulated or down-regulated, respectively, in T$_{FC}$ compared to non-T$_{FC}$ cells. Selected differentially expressed genes were highlighted in red (up-regulated) or blue (down-regulated). **(B-E)** FACS histograms show the expression of indicated proteins in naïve (grey), CXCR5$^+$ T$_{FC}$ (red) and CXCR5$^-$ non-T$_{FC}$ (blue) cells as gated in (B) at D8 p.i. GMFI: geometric mean fluorescence intensity. **(F)** *Ex vivo* killing of LCMV gp$_{33-41}$ peptide-pulsed splenocytes by naïve, CXCR5$^+$ T$_{FC}$ or CXCR5$^-$ non-T$_{FC}$ P14 cells purified at D8 p.i. Each symbol represents one mouse; bars represent means. Data are representative of two (B-E) to three (F) independent experiments. **P < 0.01, as calculated by one-way ANOVA followed by Sidak's multiple comparison test.
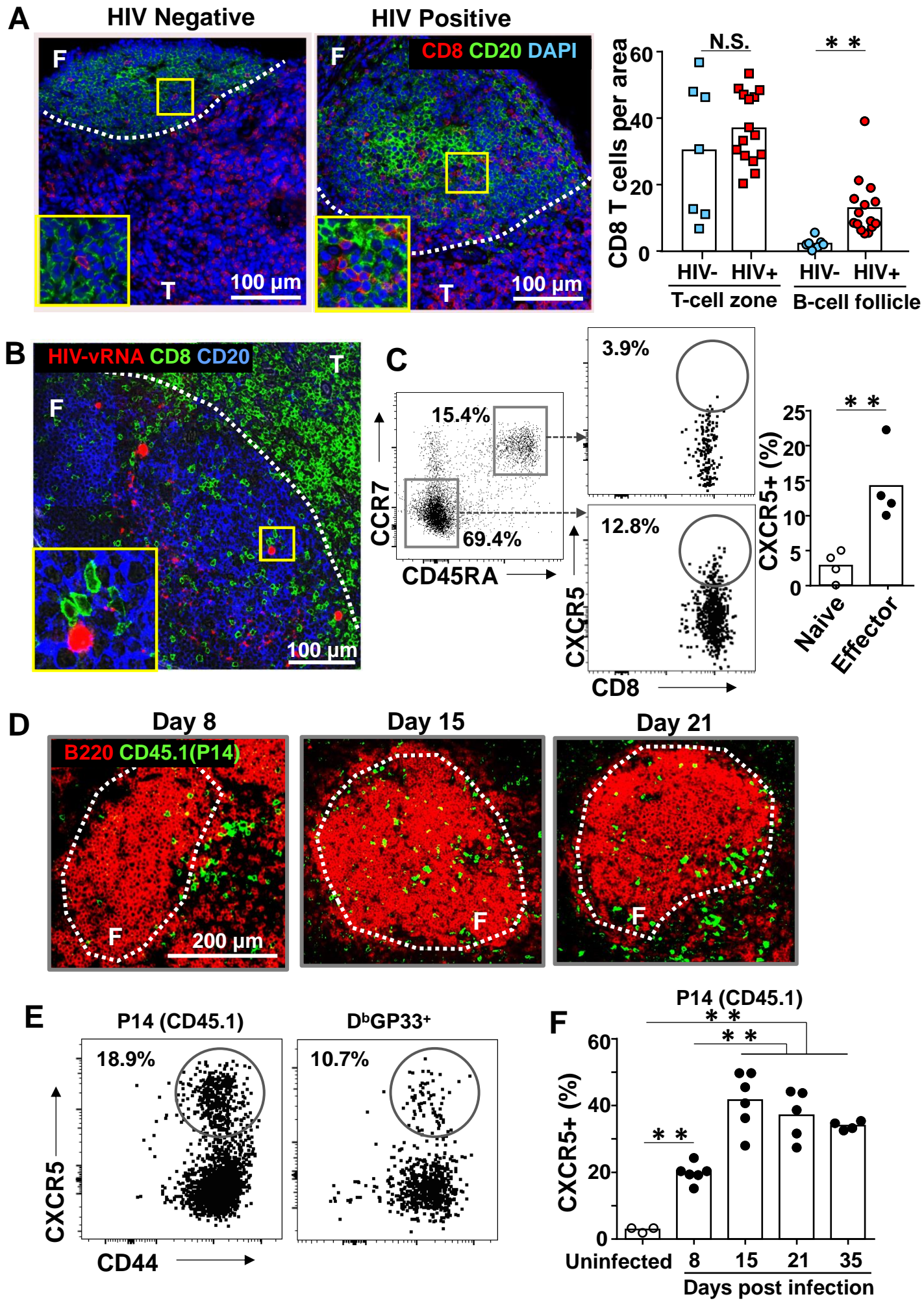
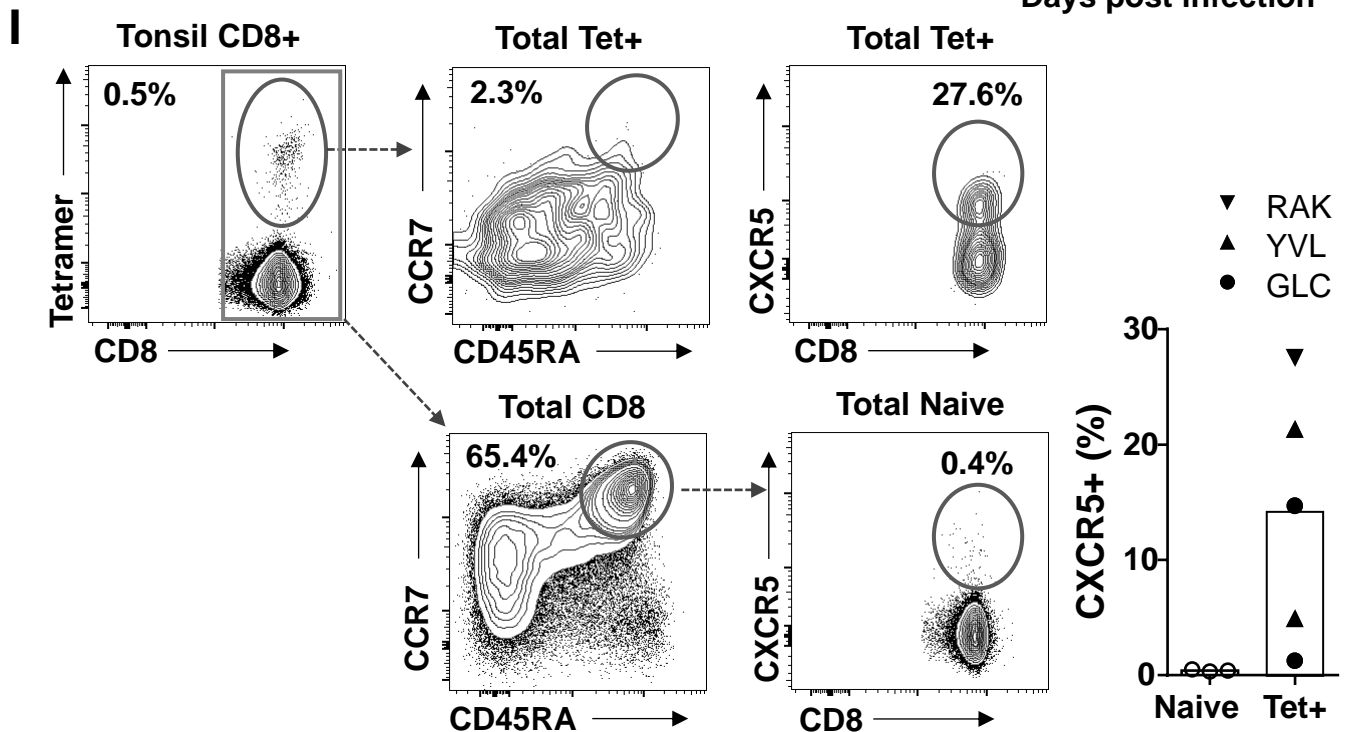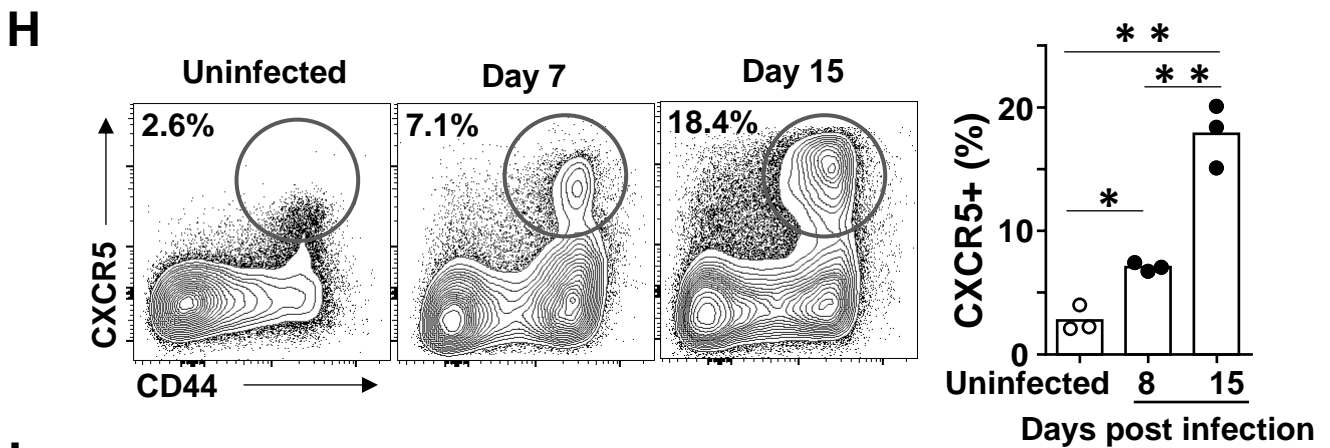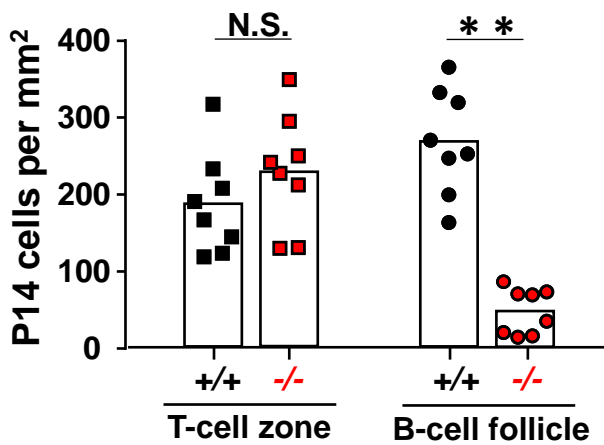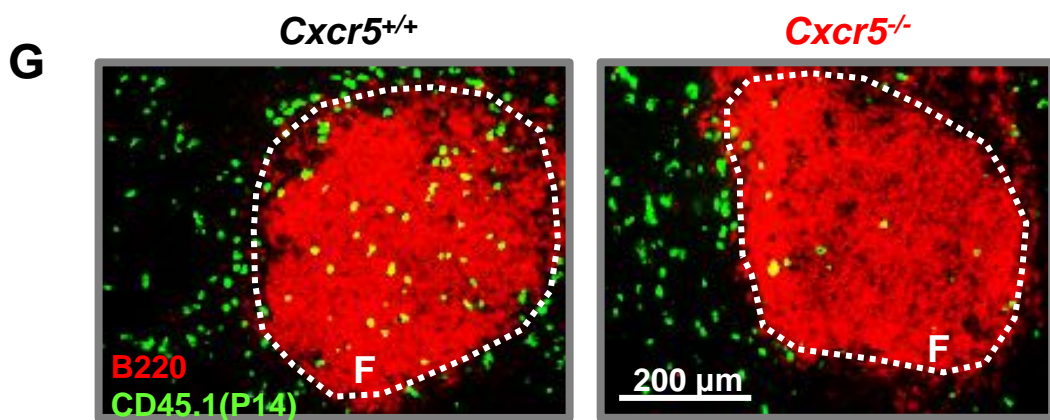**Figure 4: Transcriptional regulation of T$_{FC}$ differentiation. (A, B)** Expression of transcriptional regulators Bcl6, Tcf1, Id3, Blimp1 and Id2 as determined by intracellular staining (Bcl6 and Tcf1) or GFP reporter (Id3, Blimp1 and Id2). FACS histograms show the expression of indicated genes in naïve CD8 (grey), CXCR5$^+$ T$_{FC}$ (red) and CXCR5$^-$

non-T$_{FC}$ (blue) cells at D8 p.i. **(C-D)** Congenically marked P14 cells were transduced with a retroviral vector (RV) encoding GFP or Bcl6 (along with GFP), and transferred into recipient mice. At D8 p.i., the expression of CXCR5 on transduced cells was measured by FACS (C), and follicular positioning was quantified by IF staining (D). **(E)** Analysis of CXCR5 expression on control (*Bcl6*$^{fl/fl}$) or Bcl6-deficient (*Bcl6*$^{fl/fl}$*Cd4*^{cre}) P14 cells. **(F-I)** CXCR5 expression on antigen-specific CD8 T cells in LCMV (DOCILE)-infected chimeric mice generated from a 1:1 mixture of congenically marked control (*Prdm1*$^{fl/fl}$) or Blimp1-deficient (*Prdm1*$^{fl/fl}$*Lck*^{cre}) (F), control (*Tcf7*$^{fl/fl}$) or *Tcf7*-deficient (*Tcf7*$^{fl/fl}$*Lck*^{cre}) (G), control (*Id2*$^{fl/fl}$) or *Id2*-deficient (*Id2*$^{fl/fl}$*Lck*^{cre}) (H), and control (*Id3*$^{+/+}$) or *Id3*-deficient (*Id3*$^{gfp/gfp}$) (I) bone marrow (BM) cells on D15 p.i.. Graphs show the paired analyses of CXCR5^{+} gp$_{33}$-H-2D^{b} tetramer^{+} T$_{C}$ cells derived from WT or gene deficient donor BM cells. **(J)** P14 cells were transduced with RV or Id3-RV. At D8 p.i., the expression of CXCR5 on transduced cells was measured by FACS. **(K)** Binding of Blimp1 and E2A at the *Cxcr5* locus, as shown by ChIP-seq analysis of CD8^{+} effector T cells and total thymocytes, respectively. Binding regions, which were identified by MACS peak calling, are indicated by black rectangles below the horizontal axis. RPM: Reads per million. **(L)** WT or mutated Blimp1 binding sites at 5' upstream were cloned together with *Cxcr5*-promoter into retroviral Thy1.1-reporter constructs, followed by transduction into P14 cells. Transduced P14 cells were then injected into congenically marked recipient mice that were subsequently infected with LCMV (DOCILE). At D8 p.i., expression of Thy1.1 (% × GMFI of Thy1.1^{+}) was measured on T$_{FC}$ and non-T$_{FC}$ P14 cells. **(M)** Blimp1 and E2A binding sites at 1st intron were sequentially mutated and cloned into the same vector (L) and subsequently transduced into P14 cells. Thy1.1

expression was measured as in (L). Each symbol represents one mouse; bars represent means; lines represent paired samples. Data are representative of at least two independent experiments. *P < 0.05, **P < 0.01, as calculated by Mann-Whitney's U-test (C, D, E, J, L), one-way ANOVA (M), two-way ANOVA (D) and RM two-way ANOVA (F, G, H, I) followed by Sidak's multiple comparison tests.
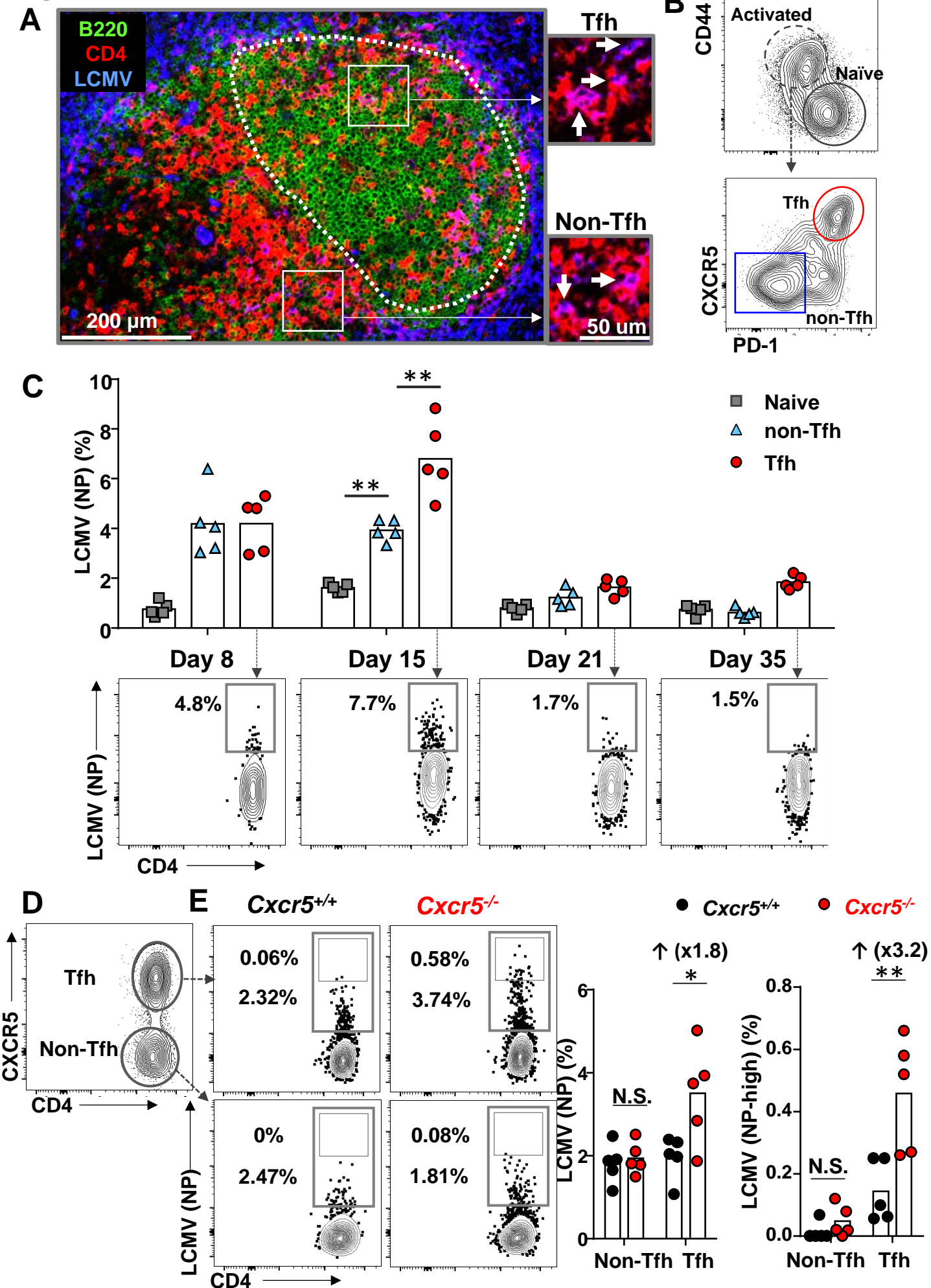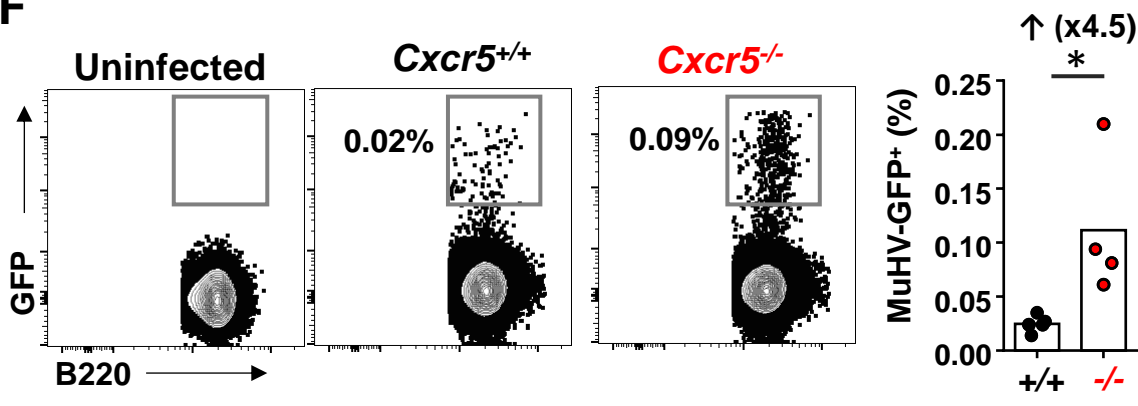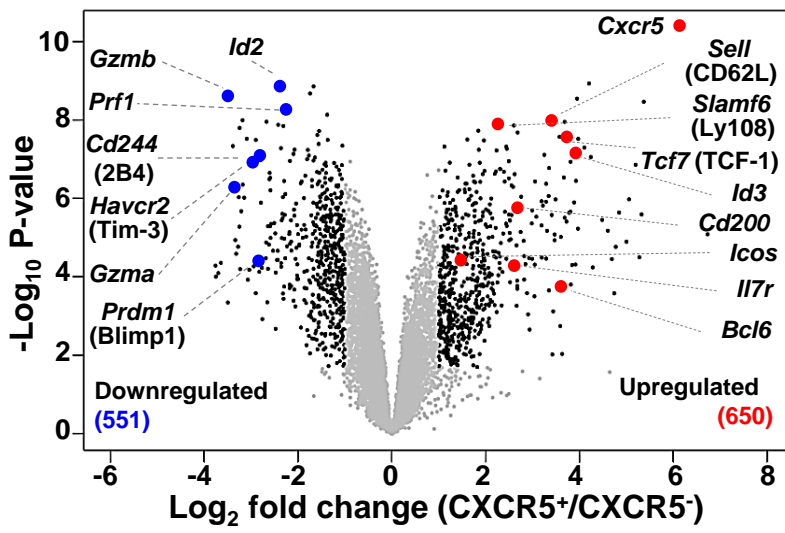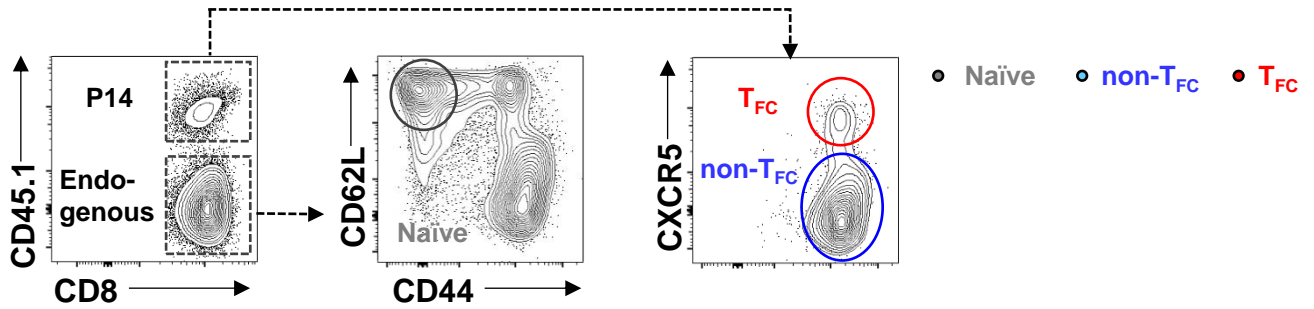
Figure 1

A HIV Negative | HIV Positive
CD8 CD20 DAPI
F, T, 100 μm

CD8 T cells per area
N.S. | **
HIV- HIV+ | HIV- HIV+
T-cell zone | B-cell follicle

B HIV-vRNA CD8 CD20
F, T, 100 μm

C
CCR7 / CD45RA
15.4%
69.4%
3.9%
12.8%
CXCR5 / CD8

CXCR5+ (%)
**
Naive | Effector

D Day 8 | Day 15 | Day 21
B220 CD45.1(P14)
F, 200 μm

E P14 (CD45.1) | D^bGP33+
18.9% | 10.7%
CXCR5 / CD44

F P14 (CD45.1)
CXCR5+ (%)
**
**
**
Uninfected 8 15 21 35
Days post infection

G

Cxcr5^{+/+} *Cxcr5*^{-/-}

B220
CD45.1(P14)

200 μm

F   F

N.S.   * *

P14 cells per mm²

400
300
200
100
0

+/+   -/-   +/+   -/-
T-cell zone   B-cell follicle

H

Uninfected   Day 7   Day 15

CXCR5
CD44

2.6%   7.1%   18.4%

* *
* *
*

CXCR5+ (%)

20

10

0

Uninfected   8   15
Days post infection

I

Tonsil CD8+   Total Tet+   Total Tet+

Tetramer
CD8

0.5%

CCR7
CD45RA

2.3%

CXCR5
CD8

27.6%

Total CD8   Total Naive

CCR7
CD45RA

65.4%

CXCR5
CD8

0.4%

RAK
YVL
GLC

CXCR5+ (%)

30

20

10

0

Naive   Tet+

Figure 2

F

Uninfected　　Cxcr5^{+/+}　　Cxcr5^{-/-}

GFP

B220

0.02%　　0.09%

↑ (x4.5)
*

MuHV-GFP$^+$ (%)

+/+　　-/-

Figure 3

Figure 4

A Bcl6 · Tcf1 · Id3-GFP

Legend: ● Naïve · ● non-T_FC · ● T_FC

B Blimp1-GFP · Id2-GFP

C RV · Bcl6 · 13.2% · 54.6% · CXCR5+ (%) · RV · Bcl6 · **

D RV · RV-Bcl6 · B220 · CD45.1(P14) · 200 μm

↑ (x2.5) · ↑ (x10.2) · P14 cells per mm² · RV · Bcl6 · RV · Bcl6 · T cell zone · B cell follicle · ** · ** · Ratio (follicular/non-follicular) · RV · Bcl6 · **

E *Bcl6*^+/+ · *Bcl6*^Cd4-Cre · 13.2% · 4.0% · CXCR5+ (%) · +/+ · -/- · **

F *Blimp1*^+/+ · *Blimp1*^Lck-Cre · 12.6% · 49.3% · CXCR5+ (%) · N.S. · ** · +/+ +/+ · +/+ -/-

G *Tcf7*^+/+ · *Tcf7*^Lck-Cre · 13.0% · 5.9% · CXCR5+ (%) · N.S. · ** · +/+ +/+ · +/+ -/-

H *Id2*^+/+ · *Id2*^-/- · 14.8% · 27.8% · CXCR5+ (%) · N.S. · * · +/+ +/+ · +/+ -/-

I

Id3$^{+/+}$ Id3$^{-/-}$

CXCR5

CD44

14.0%   40.9%

N.S.   **

CXCR5+ (%)

80
60
40
20

+/+ +/+   +/+ -/-

J

RV   Id3

CXCR5

CD44

11.6%   1.4%

**

CXCR5+ (%)

20
15
10
5

RV   Id3

K

1st Intron   5' Upstream

3

Blimp1

Binding (RPM)

40

E2A

Bcl9l   *Cxcr5*

10 kb

L

T$_{FC}$ non-T$_{FC}$

Thy1.1 expression (% x GMFI)

300

200

100

0

N.S.   **

Blimp1^{WT} Blimp1^{Mut} Blimp1^{WT} Blimp1^{Mut}

M

T$_{FC}$ non-T$_{FC}$

Thy1.1 expression (% x GMFI)

1800

1200

600

0

** ** ** **   ** * ** *

E2A^{WT}Blimp1^{WT} E2A^{MUT}Blimp1^{WT} E2A^{WT}Blimp1^{MUT} E2A^{MUT}Blimp1^{MUT} E2A^{WT}Blimp1^{WT} E2A^{MUT}Blimp1^{WT} E2A^{WT}Blimp1^{MUT} E2A^{MUT}Blimp1^{MUT}

Supplementary figure 1

**Figure S1: Follicular entry of polyclonal T$_C$ cells in LCMV infection.**
Staining of anti-CD3 (red), anti-CD8 (green) and anti-B220 (blue) of splenic sections from uninfected mice or mice at day 8 post-infection (p.i.). Higher magnification of B cell follicles from mice at day 8 p.i. was shown (lower panel). CD8$^+$ T cells (yellow) are identified by co-staining with anti-CD3 and anti-CD8. Data are representative of 2 independent experiments.

Supplementary figure 2

A
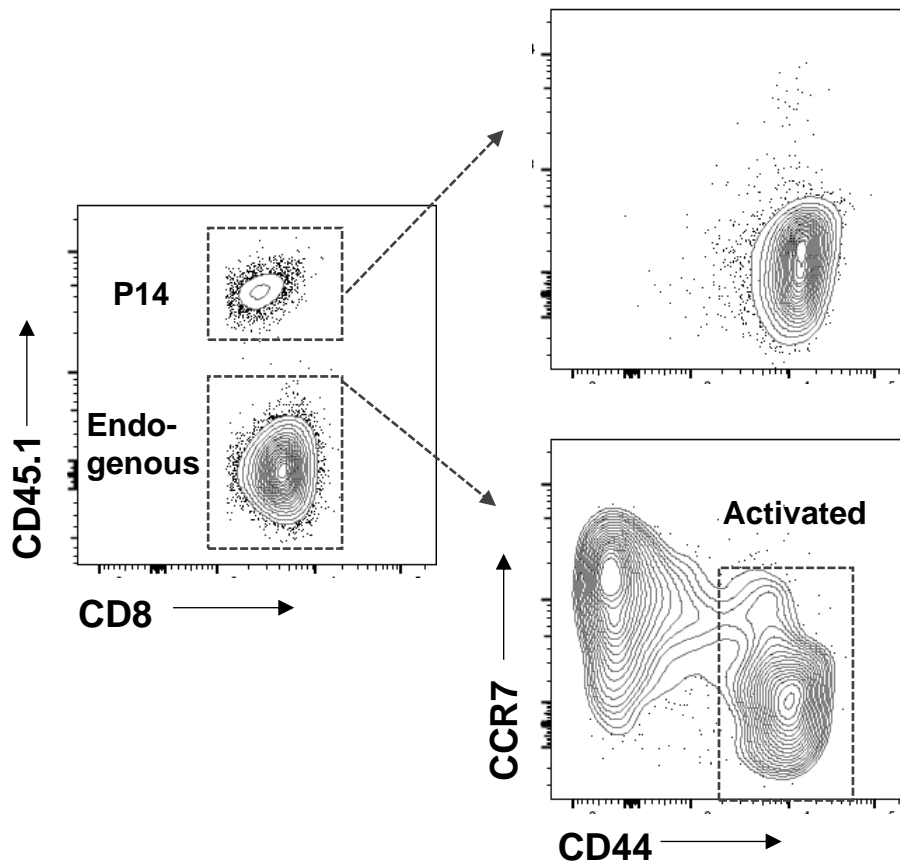
B
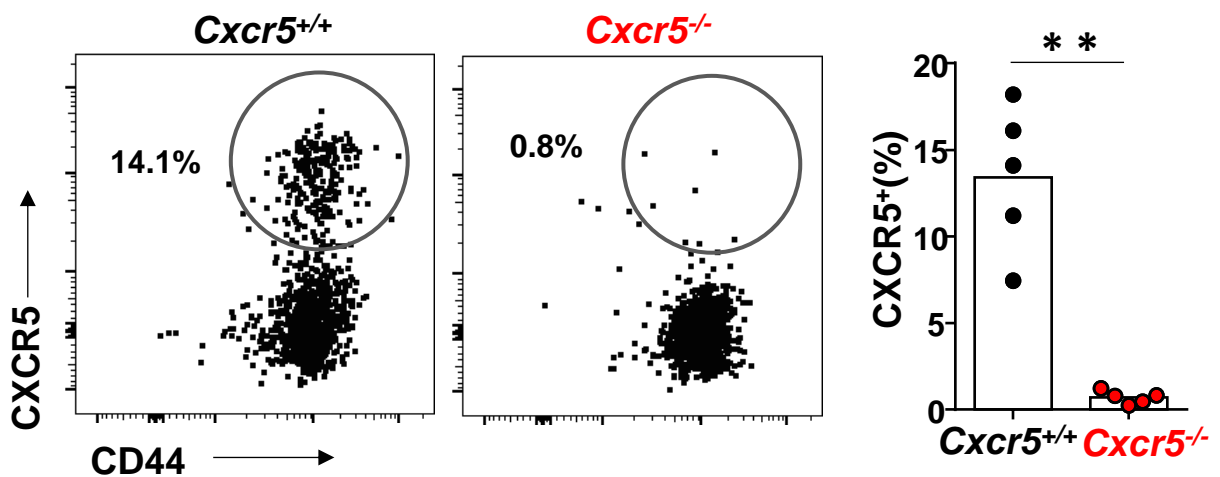
Figure S2: The expression of CXCR5 and CCR7 on CD8+ T cells.
(**A**) CD45.1+ P14 cells were adoptively transferred into congenically marked (CD45.2) wildtype mice, which were then infected with LCMV (DOCILE). Flow cytometric analysis of CCR7 expression on P14 cells or endogenous activated CD44+ T_C cells at day 8 p.i.
(**B**) CD45.1+ *CXCR5+/+* or *CXCR5-/-* P14 cells were adoptively transferred into congenically marked (CD45.2) wildtype mice, which were then infected with LCMV (DOCILE). Flow cytometric analysis of CXCR5 expression on P14 cells at day 8 p.i. Each symbol represents one mouse, bars represent means. **P < 0.01, as calculated by Mann-Whitney *U*-test.

Supplementary figure 3
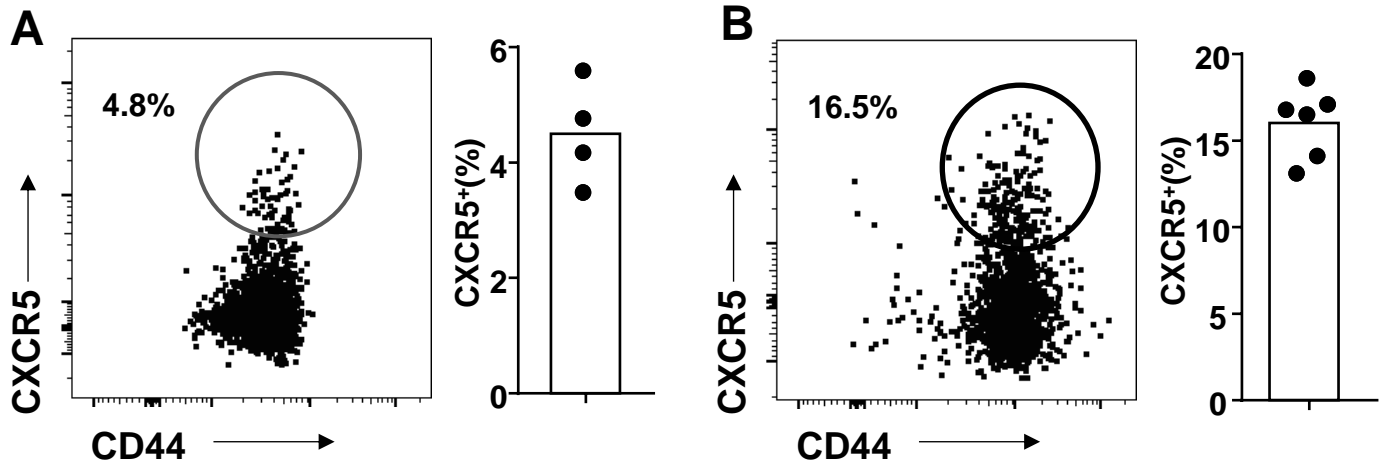
Figure S3: The expression of CXCR5 on OT-I cells after infection or immunization.
(**A**) OT-I cells (CD45.2) were adoptively transferred into congenically marked (CD45.1) wildtype mice, which were then intravenously infected with OVA-expressing influenza virus. Flow cytometric analysis of CXCR5 expression on OT-I cells in spleens at day 10 p.i.
(**B**) OT-I cells (CD45.2) were adoptively transferred into congenically marked (CD45.1) wildtype mice, which were then immunized subcutaneously at hock with OVA in CFA. Flow cytometric analysis of CXCR5 expression on OT-I cells in popliteal lymph nodes at day 8 post immunization. Each symbol represents one mouse, bars represent means.
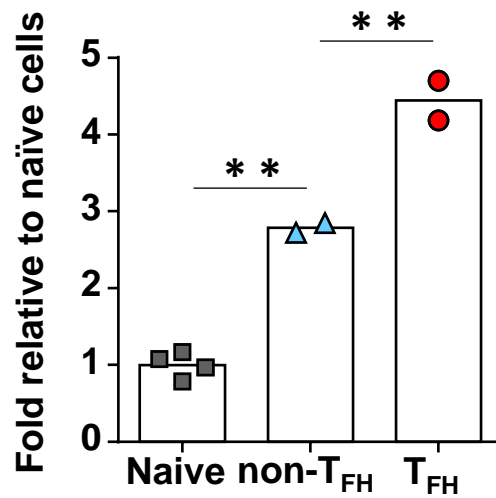
Supplementary figure 4
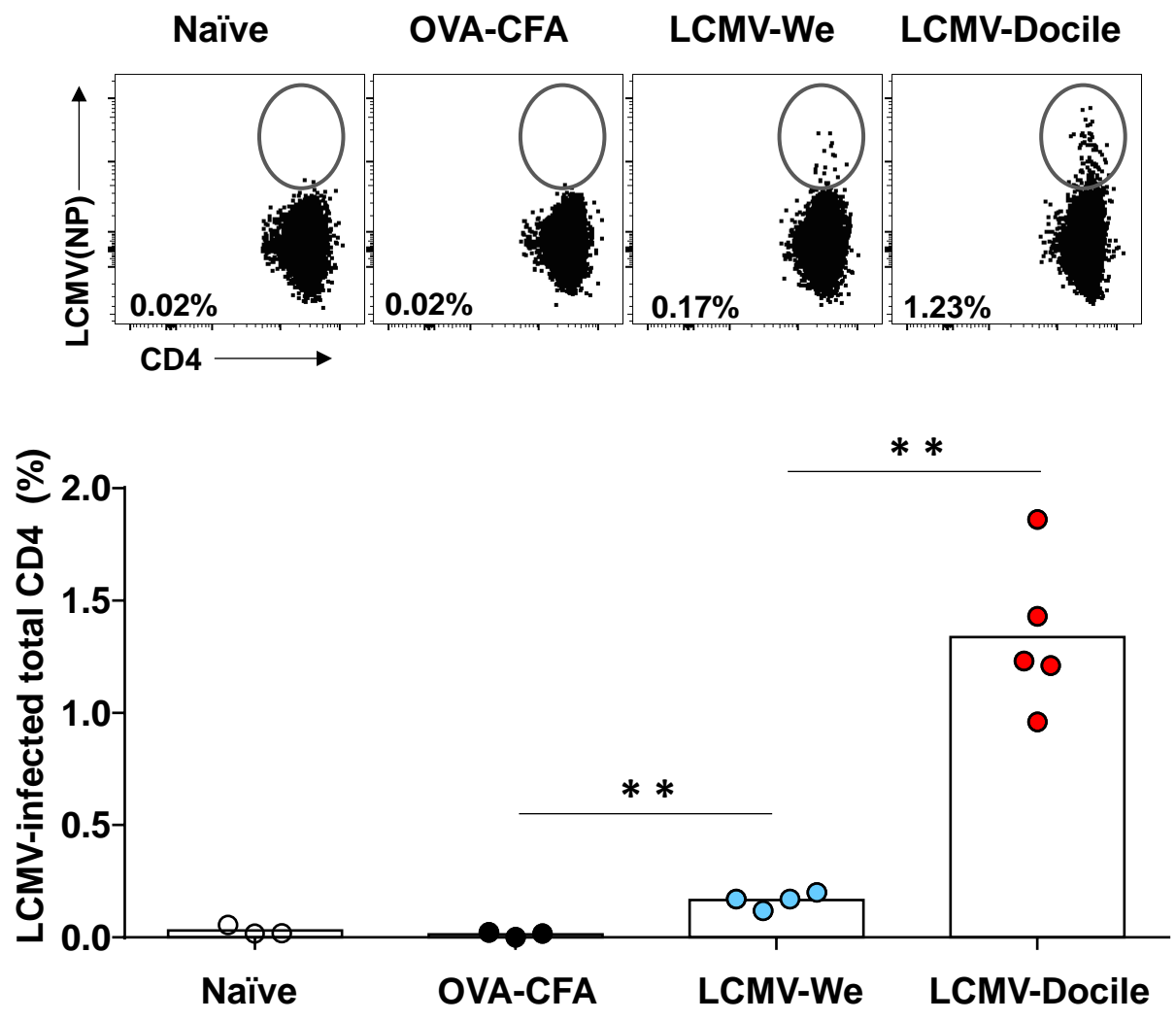
Figure S4: CD4+ T cells were significantly infected by LCMV (Docile).

Intracellular staining of LCMV NP in splenic CD4+ T cells from uninfected, day 8 post OVA-CFA immunization, day 8 p.i. with LCMV (WE) or LCMV (Docile) mice. Each symbol represents one mouse, bars represent means. **P < 0.01, as calculated by Mann-Whitney 's U-test.
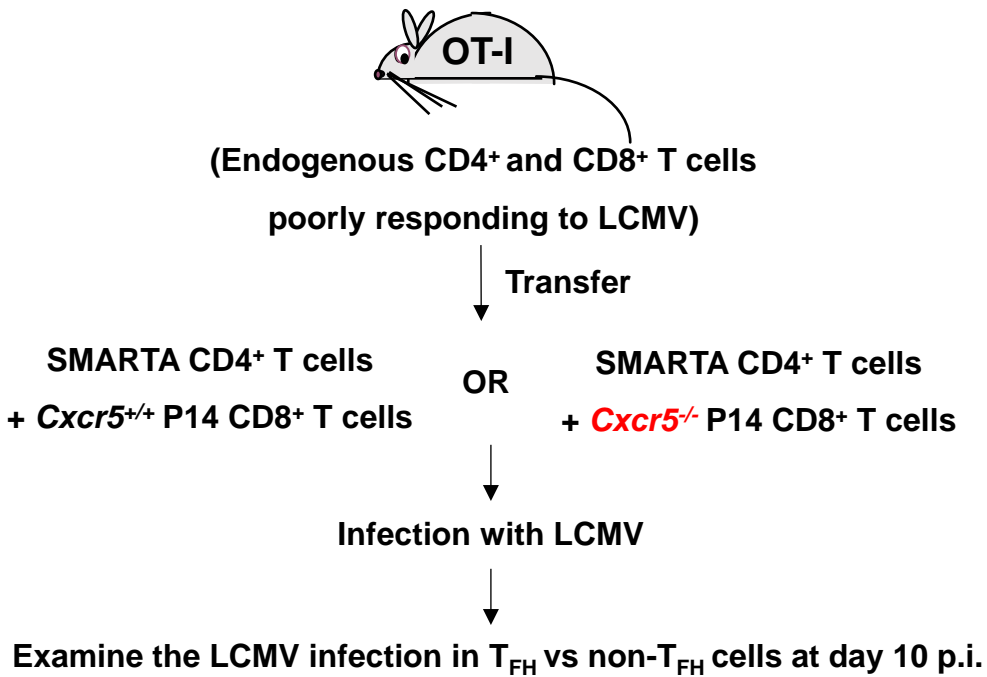
Supplementary figure 5

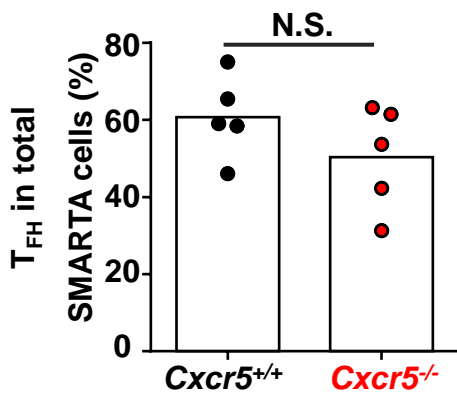**Figure S5: Higher infection in T_{FH} cells than non-T_{FH} cells.**

Eight mice were infected with LCMV (DOCILE). At day 15 p.i., T_H subsets in spleens (gated as in Fig. 2B) were purified, pooled and infection was measured by qPCR. Data are representative of two independent experiments. Each symbol represents one experimental replicate, bars represent means. **P < 0.01, as calculated by Mann Whitney's *U*-test.
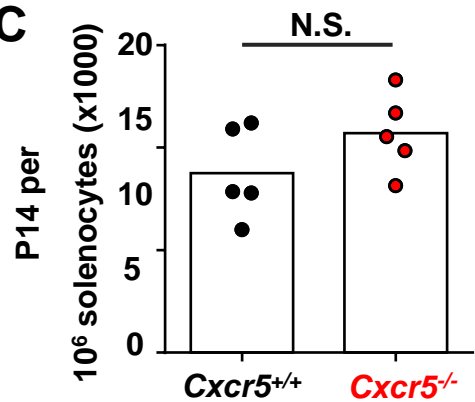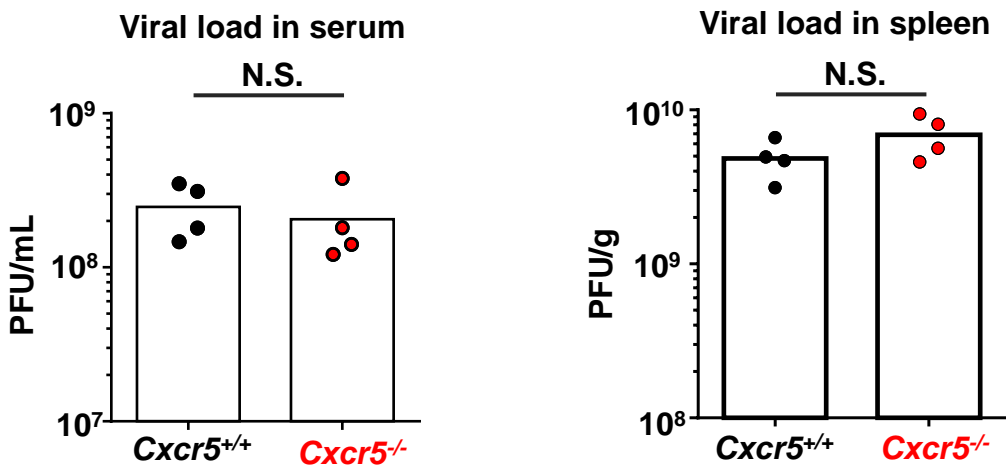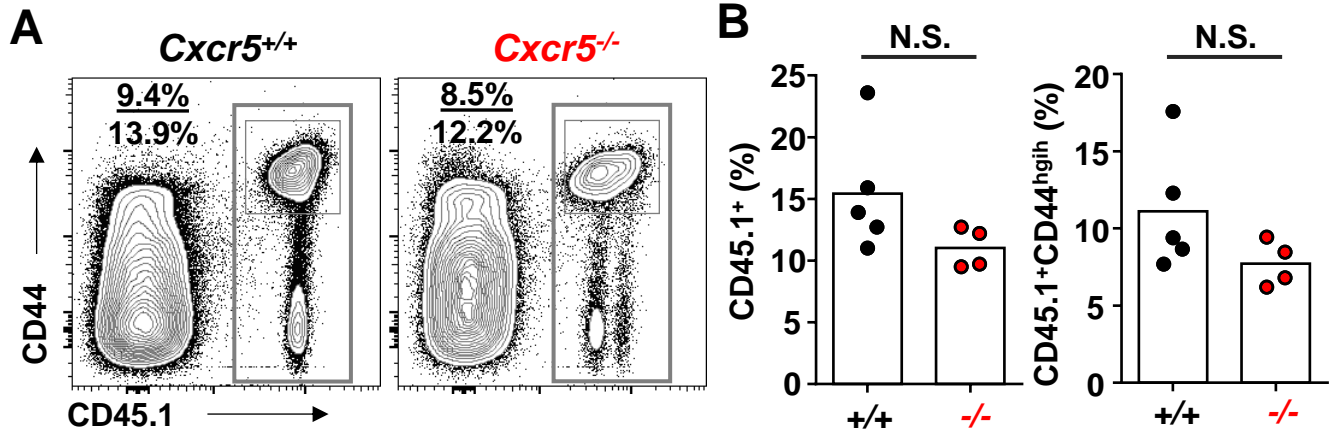
Supplementary figure 6

A

OT-I

(Endogenous CD4+ and CD8+ T cells

poorly responding to LCMV)

Transfer

SMARTA CD4+ T cells

+ *Cxcr5+/+* P14 CD8+ T cells   OR   SMARTA CD4+ T cells

+ *Cxcr5-/-* P14 CD8+ T cells

Infection with LCMV

Examine the LCMV infection in T_{FH} vs non-T_{FH} cells at day 10 p.i.

B

C

D

Viral load in serum

Viral load in spleen

Figure S6: Control of T_{FH} infection by T_{FC} cells.

(**A**) Schematic of the experiment. (**B**) Quantification of splenic T_{FH} differentiation.

(**C**) Quantification of P14 cells in spleens. (**D**) Viral loads in sera and spleens, as measured by

plaque forming assays. Data are representative of two independent experiments. Each symbol

represents one mouse, bars represent means. N.S. , not significant P > 0.05, as calculated by

Mann Whitney's *U*-test.

Supplementary figure 7

A

Cxcr5+/+   Cxcr5-/-

9.4%
13.9%

8.5%
12.2%

CD44

CD45.1

B

N.S.

CD45.1+ (%)

+/+   -/-

N.S.

CD45.1+CD44hgih (%)

+/+   -/-

Figure S7: Expansion and activation of transferred CD8+ T cells in mice infected with MuHV-4.

(**A**) Representative FACS plots showing the total CD8 T cells with transferred cells marked by congenic marker CD45.1. (**B**) Quantification of transferred cells (left) or activated transferred cells (right) in total CD8+ T cells. Data are representative of two independent experiments. Each symbol represents one mouse, bars represent means. N.S. , not significant P > 0.05, as calculated by Mann Whitney's *U*-test.
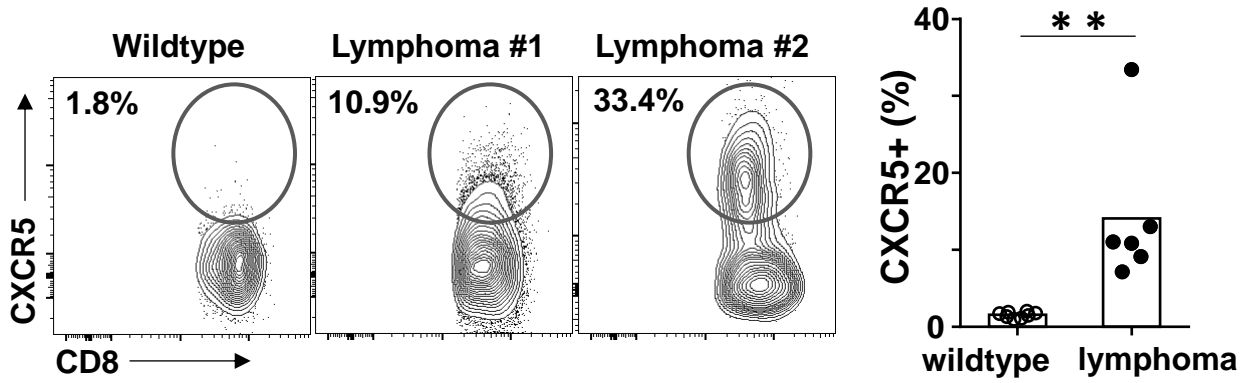
Supplementary figure 8

Figure S8: Expression of CXCR5 on CD8+ T cells in mice that developed spontaneous B-cell lymphoma. Representative FACS plots showing the expression of CXCR5 on total CD8+ T cells in WT or BCL6tg/+ mice which develop B cells lymphomas between 200-500 days of age. Each symbol represents one mouse, bars represent means. **P < 0.01, as calculated by Mann Whitney's *U*-test.

Supplementary figure 9
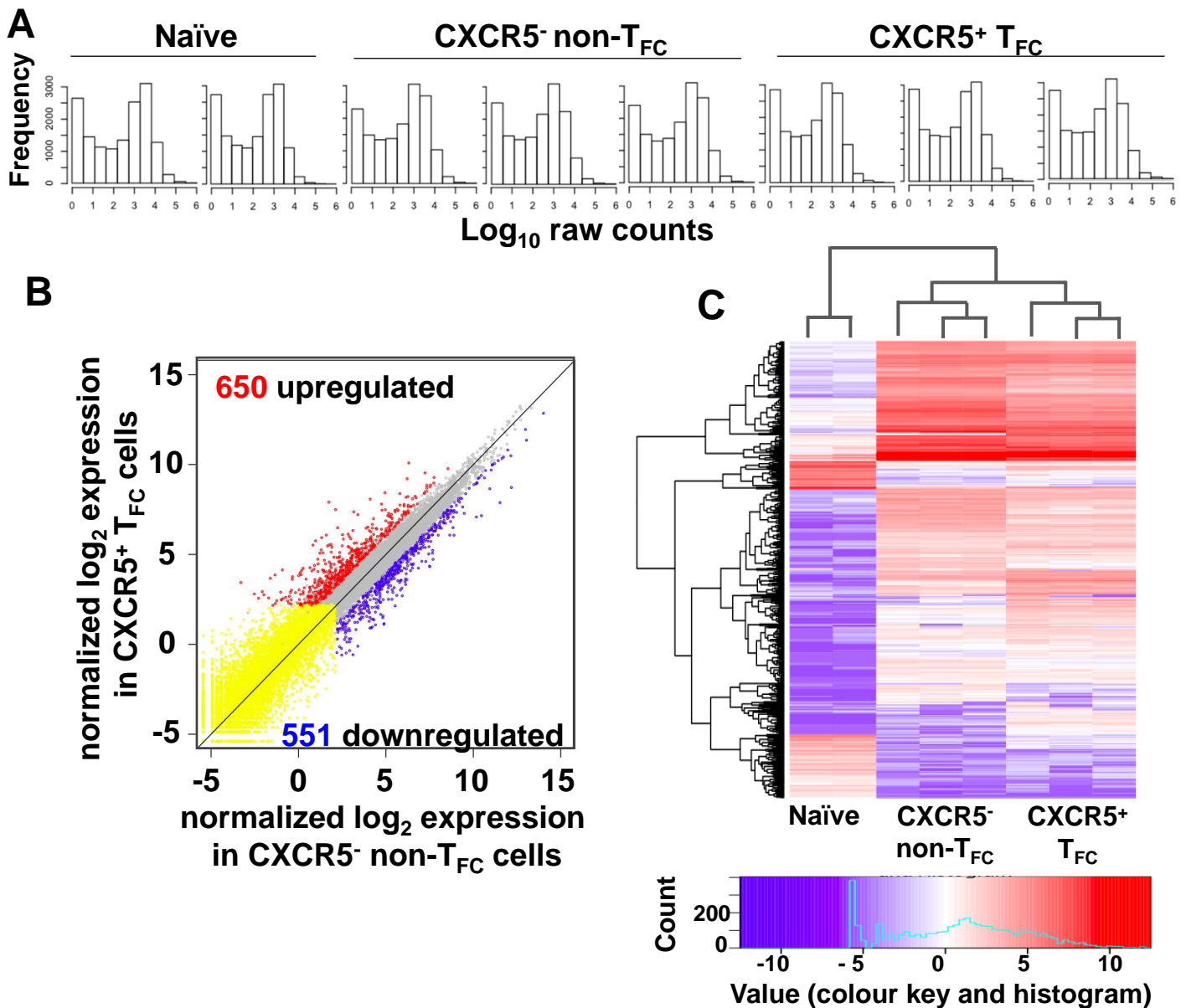
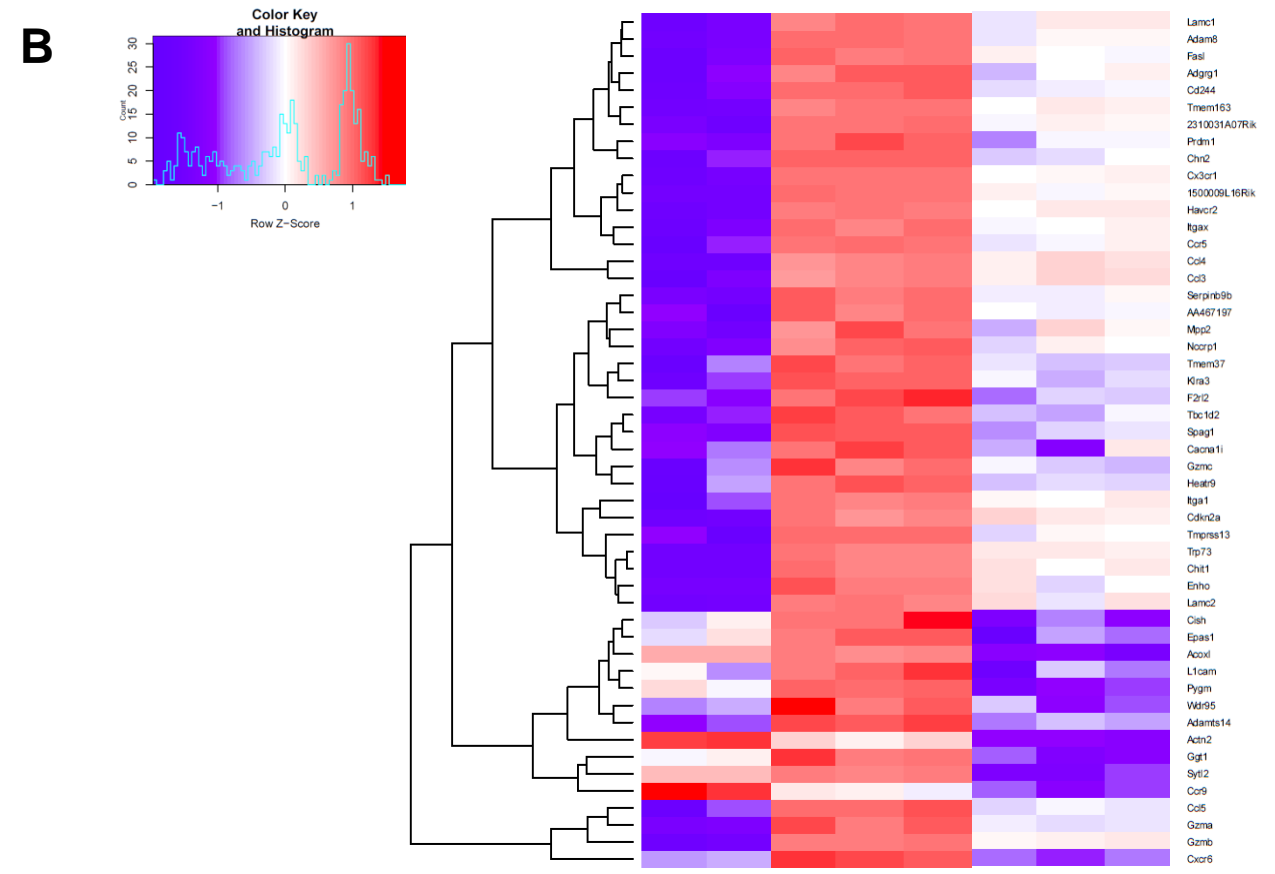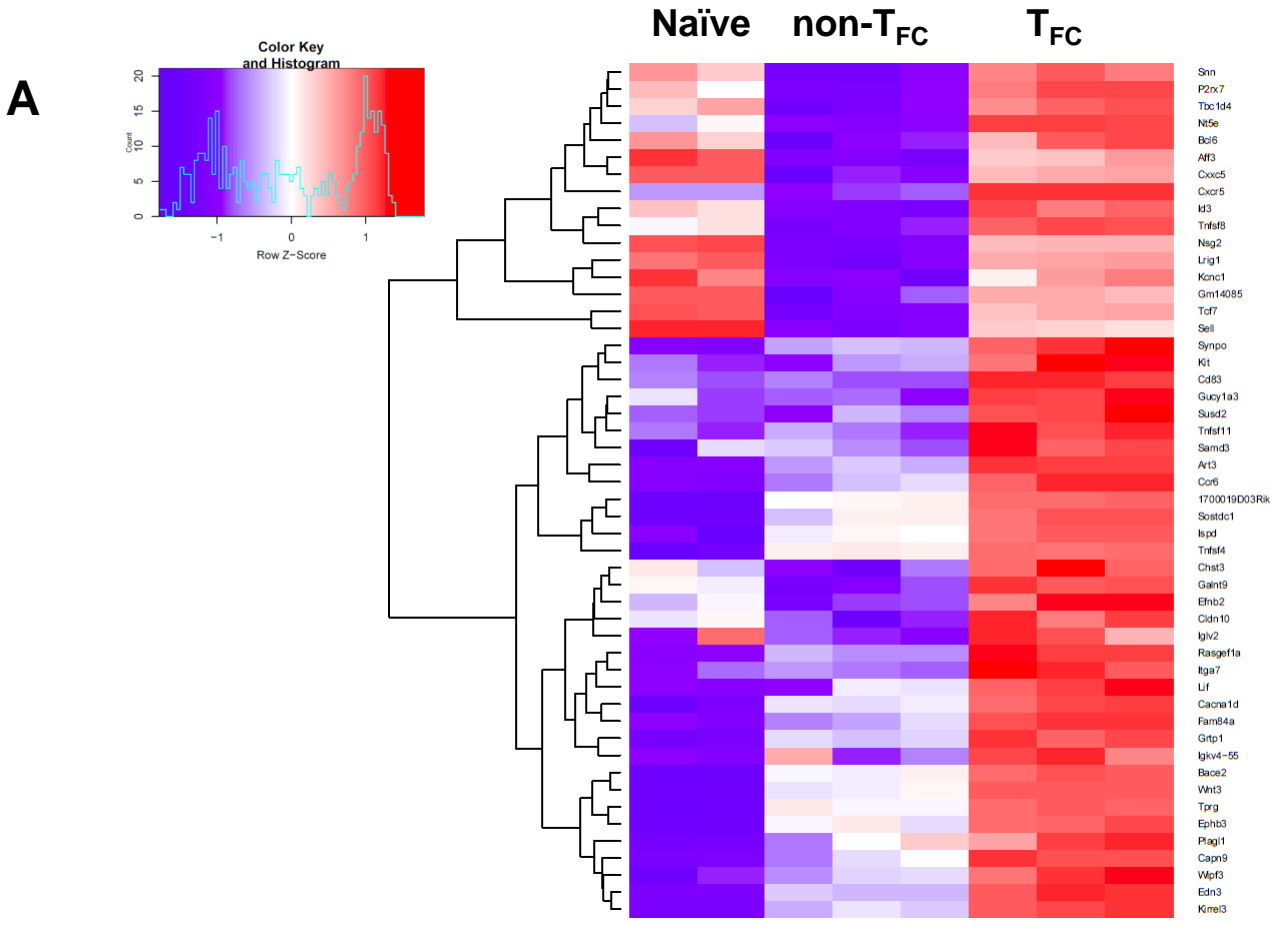

Figure S9: Transcriptomic analysis of T_{FC} cells.

CD45.1^{+} P14 cells were adoptively transferred into congenically marked (CD45.2) wildtype mice, which were then infected with LCMV (DOCILE). CXCR5^{+} T_{FC} and CXCR5^{-} non-T_{FC} P14 cells were sorted on day 8 p.i. and naïve P14 cells were subjected to RNA-seq.

(**A**) The bi-mode distribution of the $\log_{10}$ expression values of genes (count 0 excluded) shows the separation of the two peaks when $\log_{10}$ raw count is about 2. Genes with raw counts lower than 100 are considered as low/non-expressed, and filtered out for signature gene sets.

(**B**) Scatter plot of the normalized $\log_2$ data for all the 39,179 genes in CXCR5^{-} non-T_{FC} (y axis) against CXCR5^{+} T_{FC} (x axis). Yellow is for the genes that are low/non-expressed in both groups (29,423). Among 9,756 expressed genes, grey is for the genes that are not differentially expressed, red for the up-regulate genes (650), and blue for the down-regulated genes (551).

(**C**) A heatmap for normalized $\log_2$ data of the top 500 list of genes that have the largest variance across all 8 samples. The two-dimensional clustering is shown.

Supplementary figure 10

Figure S10: The top 50 up- and down-regulated genes between T$_{FC}$ and non-T$_{FC}$ cells.
Heatmaps for normalized log2 data of the top 50 lists of upregulated (**A**) or downregulated (**B**) genes.

Supplementary figure 11

A

B

C

D
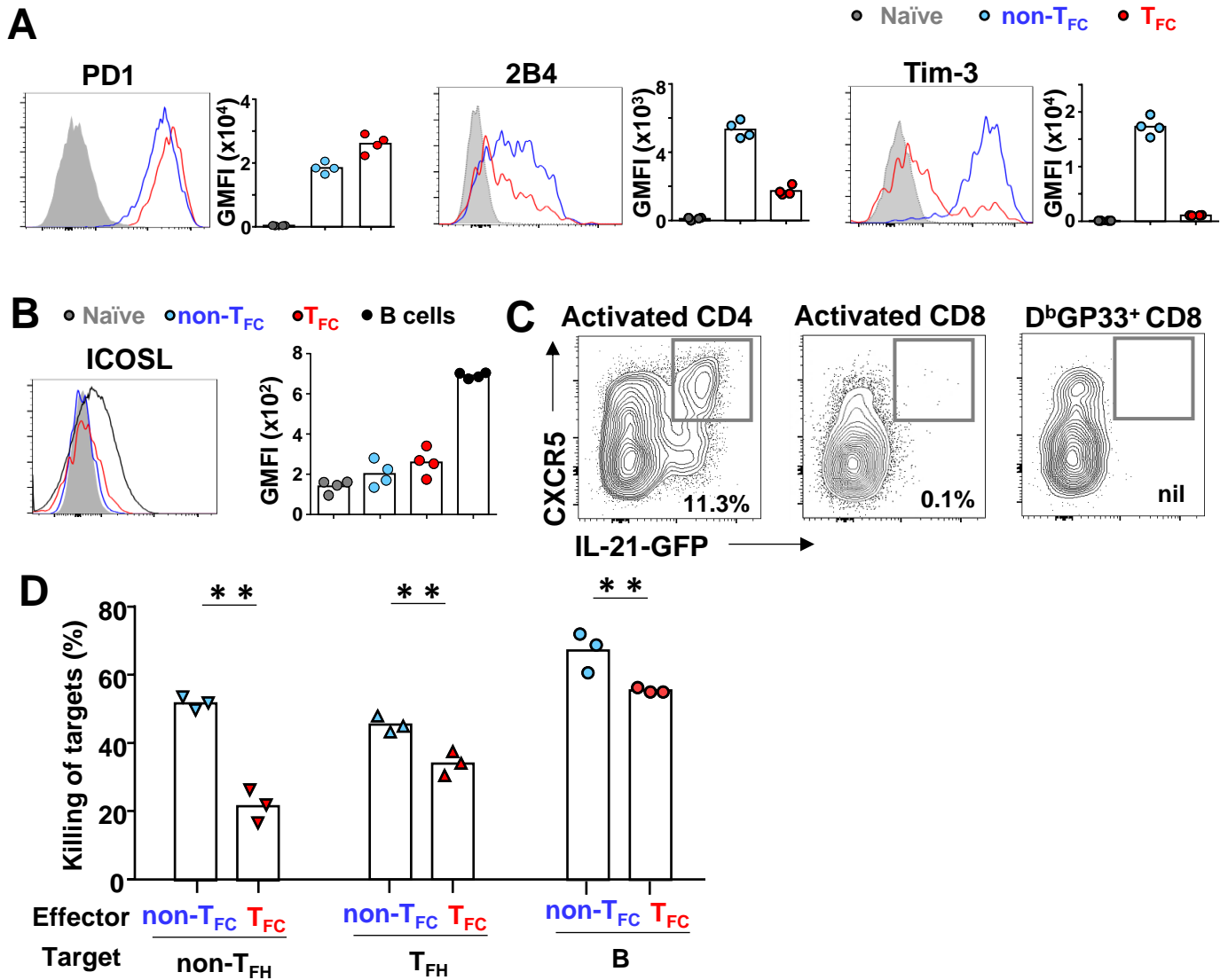
Figure S11: The expression of inhibitory receptors on T_{FC} cells.

CD45.1^{+} P14 cells were adoptively transferred into congenically marked (CD45.2) wildtype mice, which were then infected with LCMV (DOCILE). The expression of indicated proteins in naïve (grey), CXCR5^{+} T_{FC} (red), CXCR5- non-T_{FC} (blue), B220[+] B (black) cells at day 8 p.i.
(**A**) The expression of inhibitory receptors on T_{FC} cells.
(**B**) The expression of ICOSL on T_{FC} cells.
(**C**) IL-21-GFP reporter mice were infected with LCMV Docile and the expression of IL-21-GFP in indicated populations were analysed at day 15 p.i..
(**D**) *Ex vivo* killing of LCMV GP$_{33-41}$ peptide-pulsed non-T_{FH} or T_{FH} SMARTA cells, or B cells by CXCR5^{+} T_{FC} or CXCR5- non-T_{FC} P14 cells purified at day 8 p.i.
Each symbol represents one mouse (A, B and D) or one sample (C), bars represent means. GMFI: geometric mean fluorescence intensity. Data are representative of two independent experiments. **P < 0.01, as calculated by Mann-Whitney's *U*-test.

Supplementary figure 12
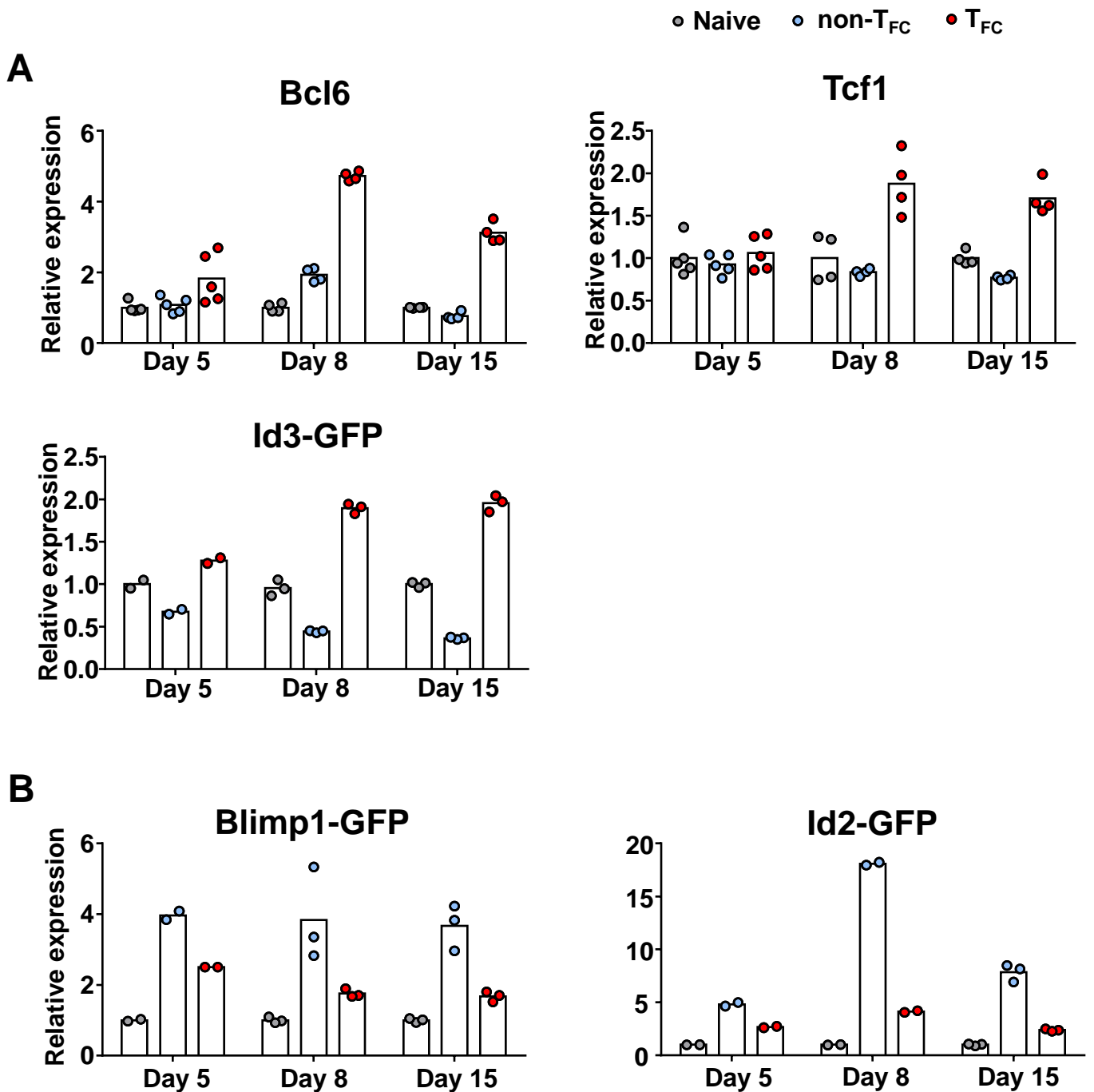
Figure S12: The expression of transcriptional regulators in T_{FC} cells.
(**A, B**) Mice were infected with LCMV (Docile) Expression of transcriptional regulators Bcl6, Tcf1, Id3, and Blimp1 and Id2 as determined using intracellular staining (Bcl6 and Tcf1) or GFP reporter (Id3, and Blimp1 and Id2) in naïve (grey), CXCR5$^+$ T_{FC} (red) and CXCR5$^-$ non-T_{FC} (blue) cells at day 8 p.i. Relative expression was calculated using GMFI divided by the average GMFI value of naïve population.

Supplementary figure 13
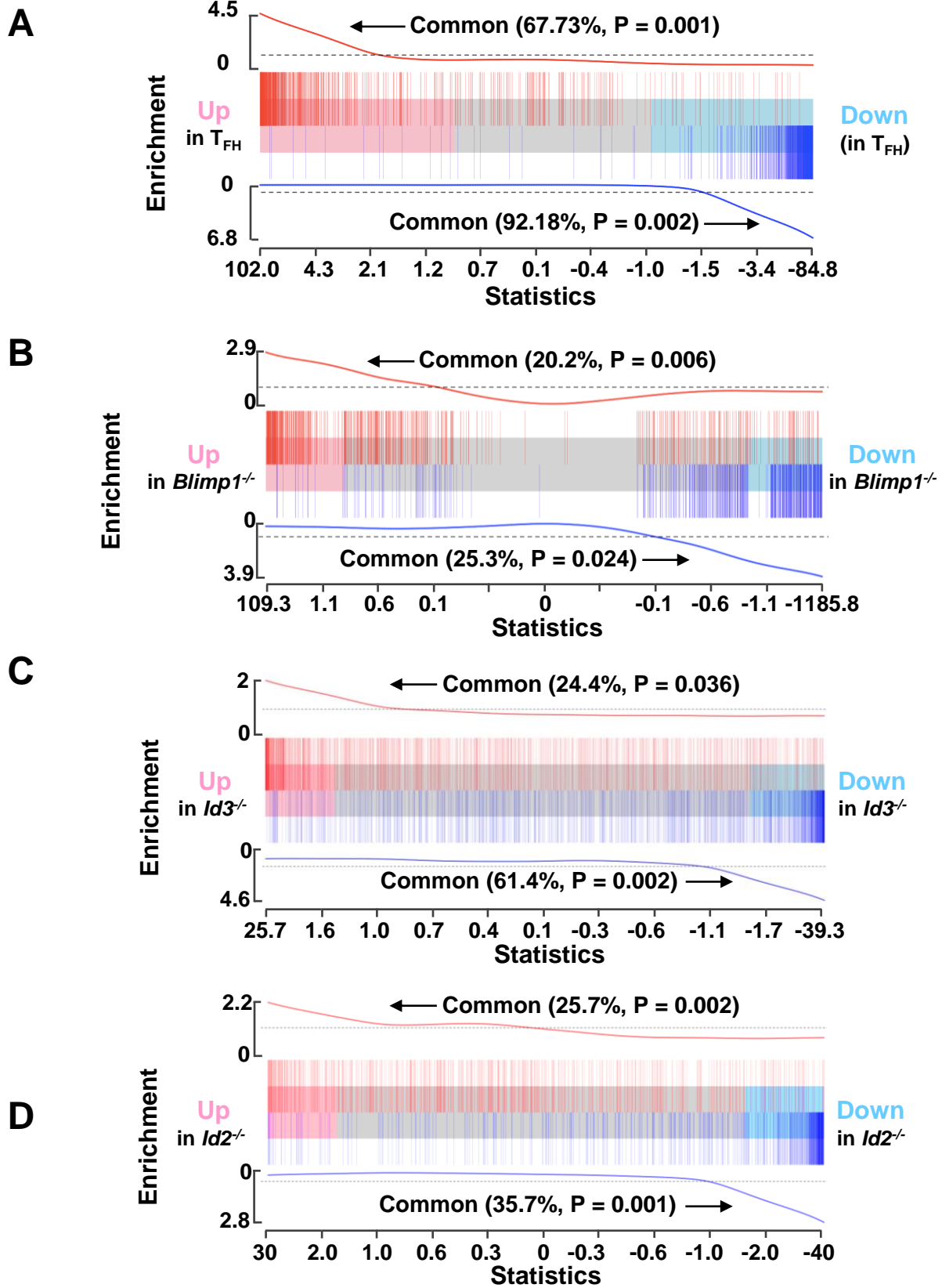
Figure S13: Enrichment analysis of the differentially expressed genes in T_FC cells
Gene set enrichment test of genes differentially expressed in T_{FC} cells as compared to non-T_{FC} cells in differentially expressed genes in T_{FH} cells as compared to non-T_{FH} cells (**A**), in Blimp1-deficient T_C cells (**B**), Id3-deficient T_C cells (**C**) and Id2-deficient T_C cells (**D**) as compared to counterpart wildtype T_C cells. Red and blue bars designate up and down-regulated genes in T_{FC} cells, respectively. Correlation of up (top) and down (bottom)-regulated genes were shown by rotation gene set test P values and the percentages.

Supplementary figure 14
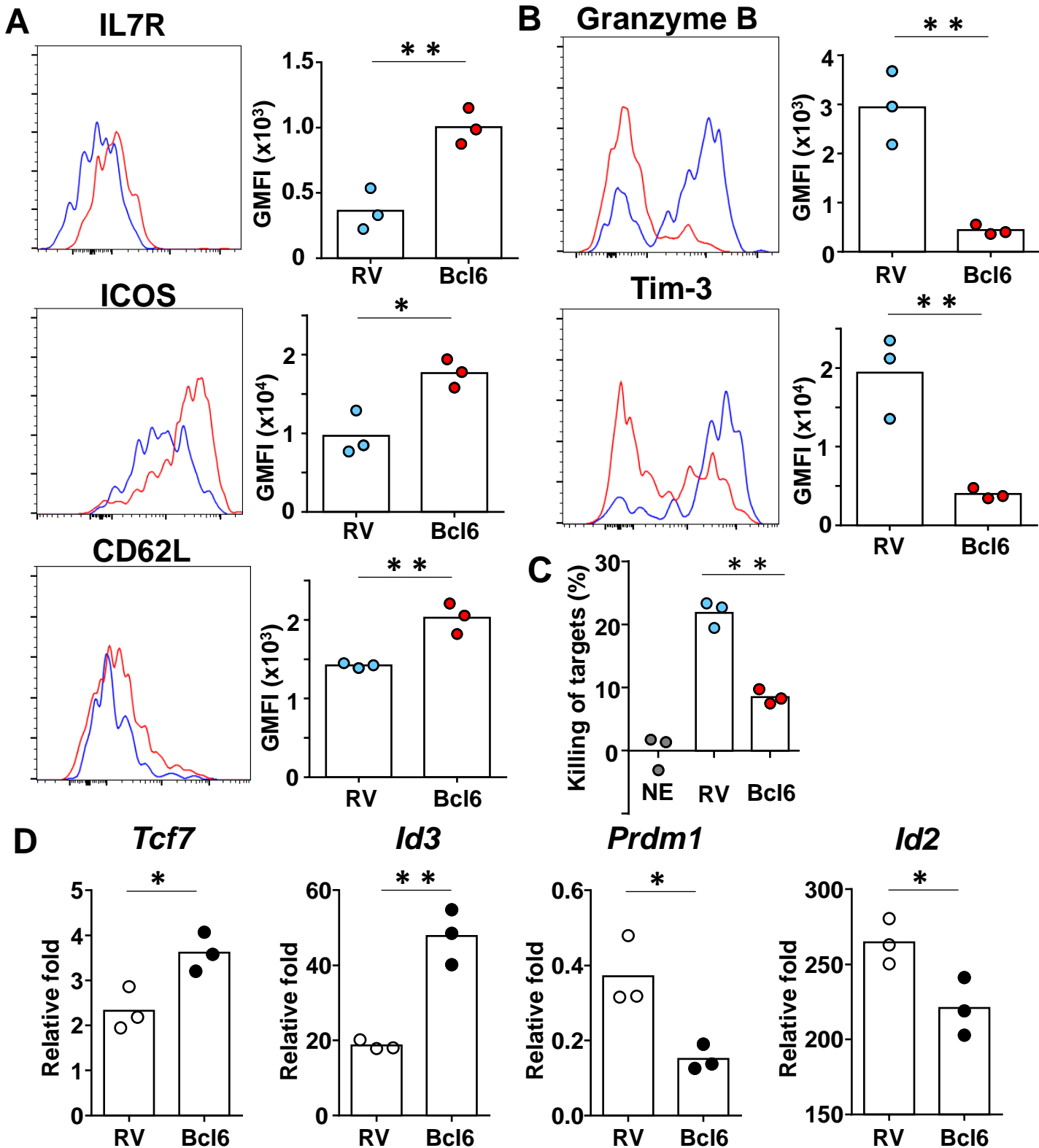
Figure S14: Bcl6 regulates the phenotype and function of T_C cells.

P14 cells were transduced with a GFP retroviral empty vector (RV) or the vector expressing Bcl6. GFP+ transduced cells were purified.

(**A, B**) Transduced cells were transferred into congenically marked recipient mice which were subsequently infected with LCMV (DOCILE). At day 8 p.i., the expression of indicated proteins on transduced cells was measured by flow cytometry.

(**C**) Transduced cells were co-cultured with LCMV gp$^{33-41}$ peptide-pulsed splenocytes and the killing of target cells were measured by flow cytometry.

(**D**) Transduced cells were isolated and the indicated genes were measured by quantitative PCR. Each symbol represents one mouse or sample, bars represent means. Data are representative of two independent experiments. *P < 0.05, **P < 0.01, as calculated by Mann Whitney's *U*-test.

Supplementary figure 15
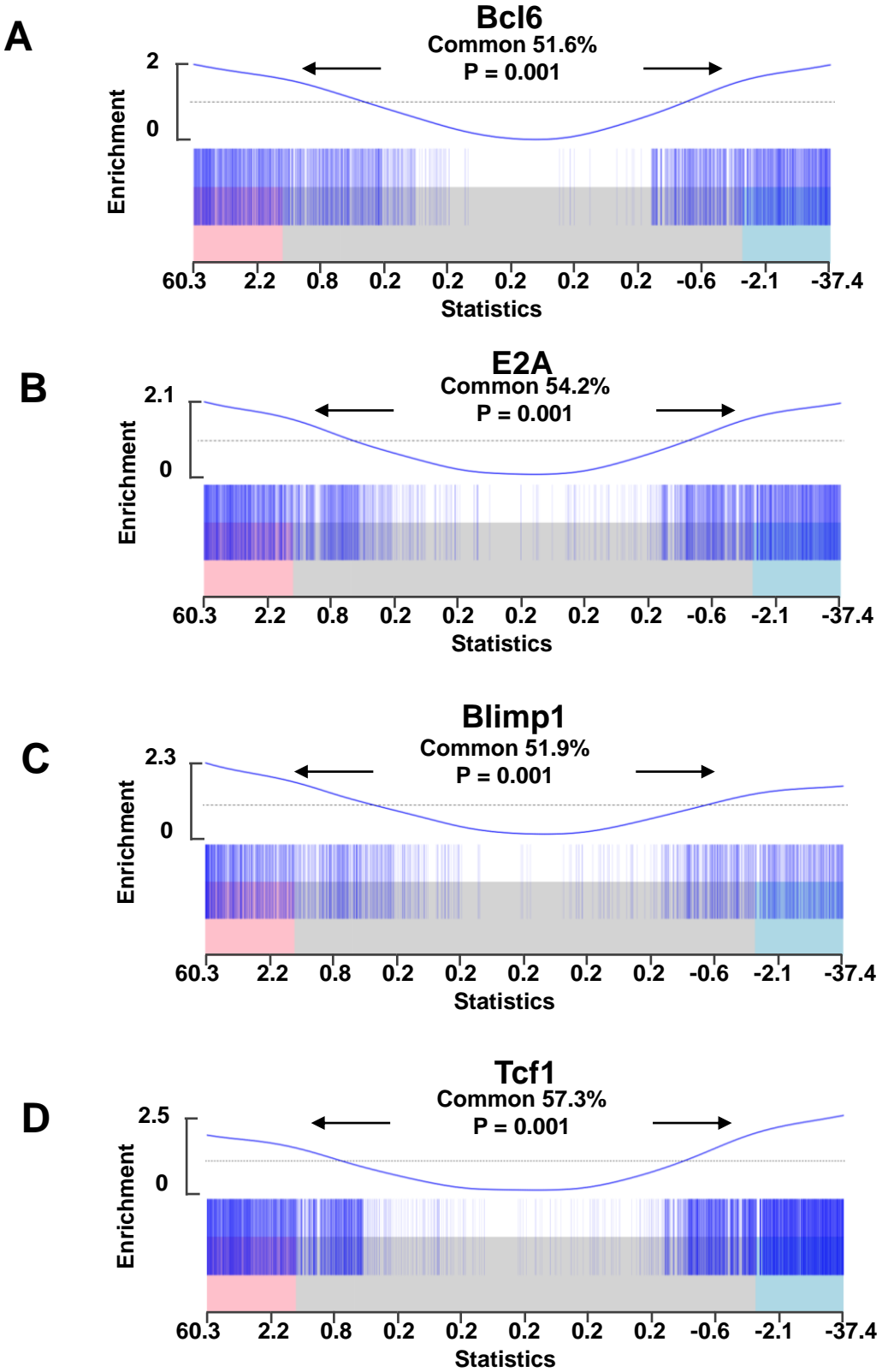
Figure S15: Correlation between transcription factor-bound genes and T_{FC} signature genes. Gene set enrichment test of genes bound by Bcl6 (**A**), Blimp1 (**B**), E2A (**C**) or Tcf1 (**D**) among transcripts differentially expressed in T_{FC} cells versus non-T_{FC} cells. Red and blue bars designate upregulated and downregulated genes in T_{FC} cells, respectively. Significant correlation of binding sites (barcode plots) with differentially expressed genes is shown by P value. Percentages show proportion of genes bound by each transcription factor that were also differentially expressed in T_{FC} vs non-T_{FC}.

Supplementary figure 16

A   5' upstream of the *Cxcr5* gene

Mouse mm9 Ch9 (+) :44,346,015 (5' → 3')

Blimp1

Human	CCTCTGCCTTGGGCCTGGCTCACTTTCACTGCTG-AGTTAGTT
Chimp	CCTCTGCCTTGGGCCCGGCTCACTTTCACTGCTG-AGTTAGTT
Mouse	CCTCCACCTGGGGCCTGGCTCACTTTCACTGCAGGACAACCAC
Rat	CCCCCACCTGGGGCCTGGTTCACTTTCACTGCAGGACAACCAC
Dog	CCTCCGCCTTGGGCCTGGTACACTTTCACTGCCGCCGATGGGT
Pig	TCTCTGTCTTGCGCCCAATTCACTTTCACTGCCGGAGACGGAG

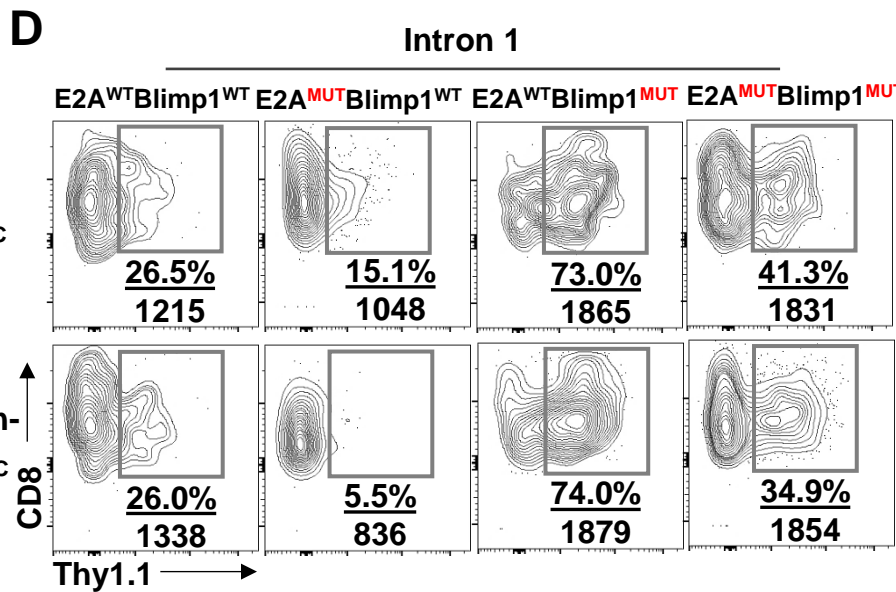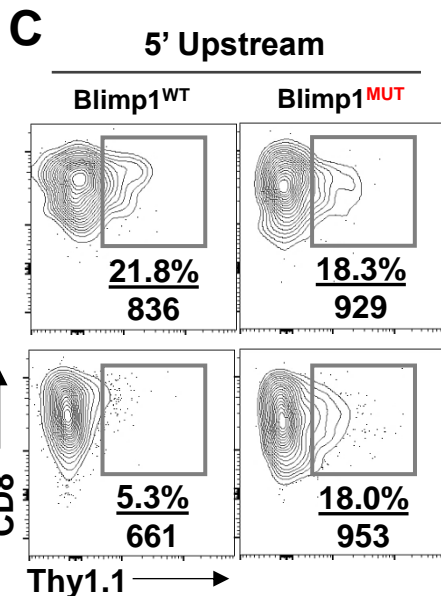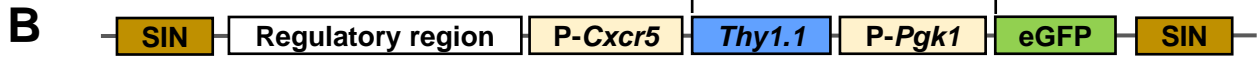Mutant sequence :   **CTAGTCCATTCT**

Intron 1 of the *Cxcr5* gene

Mouse mm9 Ch9 (+):44,323,804 (5' → 3')

E2A   **Blimp1**

Human	AGGTGCAGGGG-ACAGCTGTGAGTGAAAGGTGTGAAAACAGGCAC
Chimp	AGGTGCAGGGG-ACAGCTGTGAGTGAAAGGTGTGAAAACAGGCAC
Mouse	AGGTGCAGG---GCAGCTGTGAGTGAAAGGTATGAAAACAGGCAC
Rat	AGGTGCAGGGGGACAGCTGTGAGTGAAAGGTATGAAAACAGGCAC
Dog	AGGTGCAGG---GCAGCTGTGAGTGAAAGGTATGAAAACAGGCAC
Pig	AGGTGCATG---ACAGCTGTGAGTGAAAGGTATGAAAACAGACAC

Mutant sequence :   **GTGACC   TATGGAGAGA**

B

| SIN | Regulatory region | P-*Cxcr5* | *Thy1.1* | P-*Pgk1* | eGFP | SIN |

C   5' Upstream

Blimp1^WT   Blimp1^MUT

T_{FC}

21.8%   18.3%
836   929

non-T_{FC}

5.3%   18.0%
661   953

CD8 (y-axis)   Thy1.1 → (x-axis)

D   Intron 1

E2A^WT Blimp1^WT   E2A^MUT Blimp1^WT   E2A^WT Blimp1^MUT   E2A^MUT Blimp1^MUT

T_{FC}

26.5%   15.1%   73.0%   41.3%
1215   1048   1865   1831

non-T_{FC}

26.0%   5.5%   74.0%   34.9%
1338   836   1879   1854

CD8 (y-axis)   Thy1.1 → (x-axis)

Figure S16: Regulation of Blimp1- and E2A-binding sites in the *Cxcr5* locus.
(**A**) Genomic sequences of the *Cxcr5* genes that contain conserve putative Blimp1- or E2A-binding sites in indicated species. Mutant binding motifs used in reporter assays were indicated.
(**B**) The schematics of the retroviral vector used for *in vivo* reporter assays SIN: self-inactivating; P: promoter.
(**C, D**) P14 cells were transduced with Thy1.1-reporter constructs and GFP$^+$ cells were injected into congenically marked recipient mice followed by LCMV (DOCILE). Plots showing the representative Thy1.1 expression on T_{FC} and non-T_{FC} cells at day 8 p.i. Percentages of Thy1.1$^+$ and Thy1.1 GMFI in Thy1.1$^+$ cells are shown.

Supplementary figure 17
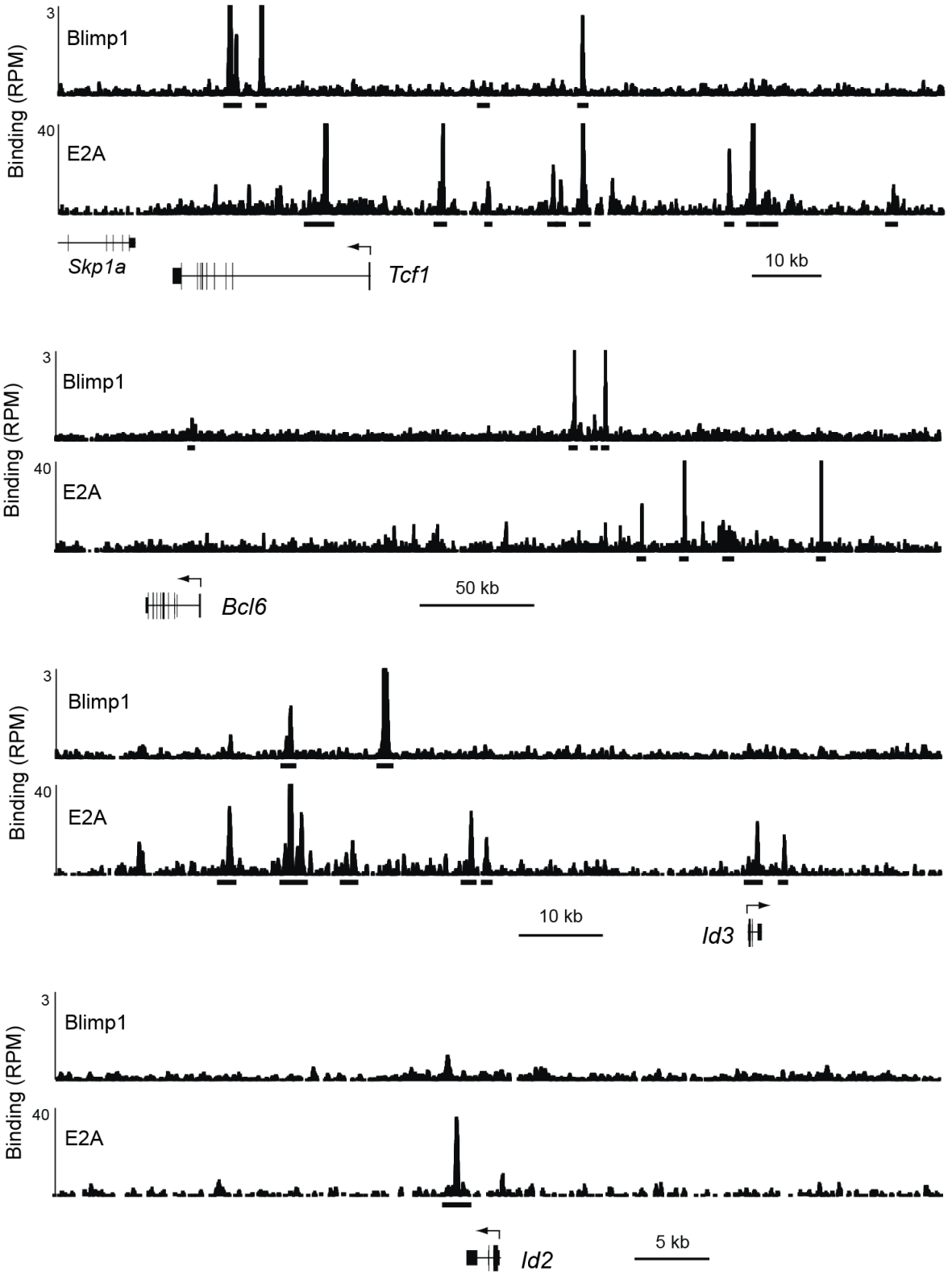
Figure S17: Binding of Blimp1 and E2A at the indicated genes. ChIP-seq analysis of Blimp1 and E2A binding was performed with CD8+ effector T cells and total thymocytes, respectively. Binding regions, which were identified by MACS peak calling, are indicated by black rectangles below the horizontal axis. RPM: Reads per million

Supplementary figure 18
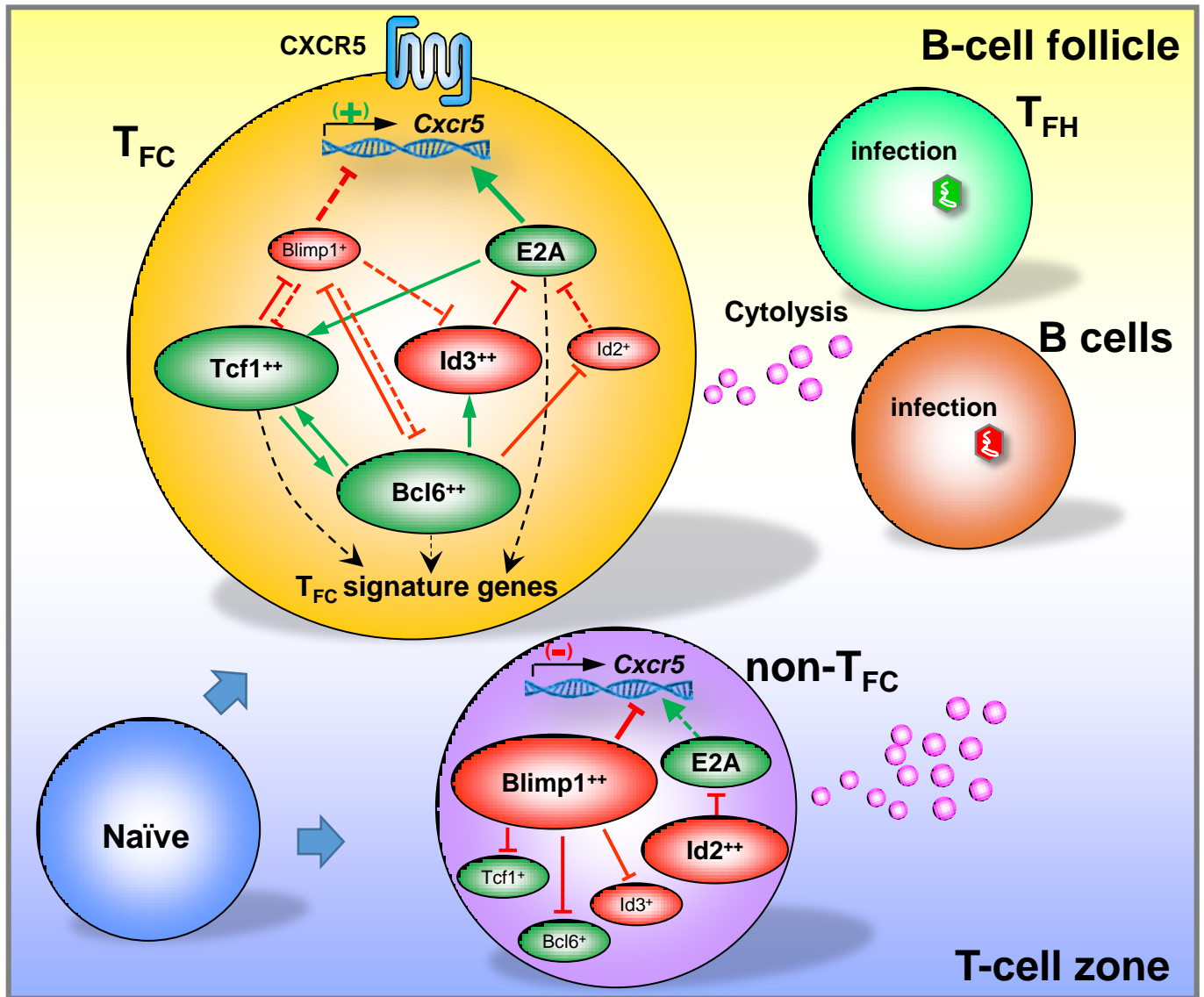
Figure 18: A working model of the differentiation and function of T_FC cells.

In persistent viral infections, T_C cells upregulate CXCR5 to enter B cell follicles and eradicate infected cells. Blimp1 and E2A directly bind to the *Cxcr5* gene locus to regulate its transcription. The differentiation of the T_{FC} population requires the transcription factors Bcl6, E2A and Tcf1 (green), whereas the transcriptional regulators Blimp1, Id3 and Id2 (red) inhibit their development. Together, these regulators form a transcriptional circuit that controls the expression of CXCR5 and directs the differentiation of T_{FC} cells.

Supplementary table 1

Table S1: Demographic and haematological characteristics of HIV-infected and control subjects.

Lymph node biopsies for immunofluorescent staining:

Patient ID	Gender	HIV Status	Date of Positive HIV Test	Biopsy Date	Age at biopsy	Years infected at Biopsy	CD4 count at Biopsy (cells/mm^3)	pVL at Biopsy (copies/mL)
2391	F	Negative	NA	3/15/2006	52	NA	837	NA
2918	M	Negative	NA	11/22/2010	63	NA	NA	NA
2966	M	Negative	NA	1/20/2011	40	NA	NA	NA
3491	F	Negative	NA	8/16/2012	53	NA	NA	NA
3820	M	Negative	NA	1/7/2014	20	NA	693	NA
3821	M	Negative	NA	1/7/2014	58	NA	NA	NA
2257	M	Positive	12/1/2003	3/8/2004	27	0.27	1,058	2,620
3447	M	Positive	10/1/2001	5/10/2012	57	10.61	560	9,800
3859	M	Positive	6/1/2011	2/10/2014	30	2.69	445	24,400
2210	F	Positive	1/1/1987	12/5/2002	43	15.93	532	167
2262	M	Positive	12/1/2003	3/8/2004	27	0.27	845	2,080
2414	M	Positive	7/18/2005	2/14/2007	30	1.57	60	4,100
3664	M	Positive	1/2/2013	3/7/2013	21	0.18	1,007	698
3709	M	Positive	9/5/2013	9/26/2013	30	0.06	453	118,000
3142	M	Positive	ND	6/2/2011	24	4*	570	62,900
3504	F	Positive	4/17/2012	9/12/2012	53	0.40	222	34,500
3620	M	Positive	9/24/2012	12/6/2012	61	0.20	335	2,100
5115	M	Positive	1/1/1982	12/9/2015	46	33.94	NA	NA

Lymph node biopsies for flow cytometry analysis:

Patient ID	Gender	HIV Status	Date of Positive HIV Test	Biopsy Date	Age at biopsy	Years infected at Biopsy	CD4 count at Biopsy (cells/mm^3)	pVL at Biopsy (copies/mL)
828063	M	Positive	NA	5/10/2016	23	NA	394	53218
828315	M	Positive	NA	5/10/2016	48	NA	128	118187
836748	M	Positive	NA	6/13/2016	42	NA	660	245526
843486	M	Positive	NA	6/14/2016	56	NA	NA	ND

*Estimated time infected

ND, not determined